

Taylor & Francis
Taylor & Francis Group

Numerical Heat Transfer, Part A: Applications
An International Journal of Computation and Methodology

ISSN: (Print) (Online) Journal homepage: www.tandfonline.com/journals/unht20

Mixed convection heat transfer and entropy generation of water inside a square vented enclosure with and without four vibrating cylinders in horizontal and vertical directions

Mushtaq F. Almensoury, Basil Mahdi Al-Srayyih, Qusay Rasheed Al-Amir, Hameed K. Hamzah, Azher M. Abed, Farooq H. Ali, Seyfettin Bayraktar, Müslüm Arıcı & Mohammad Hatami

To cite this article: Mushtaq F. Almensoury, Basil Mahdi Al-Srayyih, Qusay Rasheed Al-Amir, Hameed K. Hamzah, Azher M. Abed, Farooq H. Ali, Seyfettin Bayraktar, Müslüm Arıcı & Mohammad Hatami (2024) Mixed convection heat transfer and entropy generation of water inside a square vented enclosure with and without four vibrating cylinders in horizontal and vertical directions, Numerical Heat Transfer, Part A: Applications, 85:13, 2069-2095, DOI: 10.1080/10407782.2023.2214698

To link to this article: https://doi.org/10.1080/10407782.2023.2214698

Published online: 25 May 2023.

Submit your article to this journal

Article views: 89

View related articles

View Crossmark data

Citing articles: 1 View citing articles

Full Terms & Conditions of access and use can be found at
https://www.tandfonline.com/action/journalInformation?journalCode=unht20

NUMERICAL HEAT TRANSFER, PART A: APPLICATIONS
2024, VOL. 85, NO. 13, 2069–2095
https://doi.org/10.1080/10407782.2023.2214698

Taylor & Francis
Taylor & Francis Group

Check for updates

Mixed convection heat transfer and entropy generation of water inside a square vented enclosure with and without four vibrating cylinders in horizontal and vertical directions

Mushtaq F. Almensoury[a], Basil Mahdi Al-Srayyih[b], Qusay Rasheed Al-Amir[b,c], Hameed K. Hamzah[b,c], Azher M. Abed[c], Farooq H. Ali[b,c], Seyfettin Bayraktar[d], Müslüm Arıcı[e], and Mohammad Hatami[f]

[a]Department of Mechanical Engineering, College of Engineering, University of Al-Qadisiyah, Diwaniyah, Iraq; [b]Department of Mechanical Engineering, College of Engineering, Babylon University, Iraq; [c]Department of Air Conditioning and Refrigeration Techniques Engineering, Al-Mustaqbal University College, Babylon, Iraq; [d]Department of Marine Engineering, Faculty of Naval Architecture and Maritime, Yildiz Technical University, Istanbul, Turkey; [e]Department of Mechanical Engineering, Faculty of Engineering, Kocaeli University, Turkey; [f]Department of Mechanical Engineering, Esfarayen University of Technology, North Khorasan, Iran

ABSTRACT

The control and improvement of heat transfer in enclosures is very important in several engineering applications. In the current two-dimensional numerical study, the mixed convection and entropy generation of water flowing inside a square vented enclosure that contains four vibrating cylinders with relatively low frequencies $fr = 1$, 2, 3, 5 Hz in the vertical and horizontal directions are reported. The effects of Reynolds and Richardson numbers, vibration frequency, vibration amplitude, and the direction of the cylinders' vibration on heat transfer and entropy generation are presented for various cases. The horizontal walls of the enclosure are kept adiabatic while the vertical left and right walls are hot and cold, respectively. The linear regression analysis was used to reveal the rate of increase in the Nusselt number with the Reynolds and Richardson numbers number for each cases. Series of analyses show that the existence and the vibration of the cylinders increases heat transfer but the vibration in the horizontal direction is more effective since the top and bottom walls of the enclosure are adiabatic. It is found that the entropy generation due to heat transfer is low at the center of the enclosure. The direct relationship between the heat transfer and both Reynolds and Richardson numbers is reported. In terms of heat transfer, it is found that the critical vibration frequency and amplitude are $fr = 4$ and $A = 0.05$L and 0.075L.

ARTICLE HISTORY
Received 16 November 2022
Revised 28 April 2023
Accepted 8 May 2023

KEYWORDS
Entropy generation; mixed convection; oscillated heater; vented enclosure

1. Introduction

The improvement and control of heat transfer by convection within enclosures has attracted the attention of many researchers up to now since they play important roles in various engineering applications such as collectors used for nuclear and solar plants, ventilation of rooms, solar energy collectors, heat exchangers, electronic equipment, and other energy systems [1, 2]. As the population of the world grows and the energy demand accelerates, the need to improve the efficiency of energy systems increases. It is reported that the global energy demand will increase by approximately 50% in the next 20 years due to fast rise in global population [3]. Despite all the

CONTACT Seyfettin Bayraktar sbay@yildiz.edu.tr Department of Marine Engineering, Faculty of Naval Architecture and Maritime, Yildiz Technical University, 34349 Istanbul, Turkey.

© 2023 Taylor & Francis Group, LLC

Nomenclature

A	amplitude, m
Be	Bejan number
C_p	specific heat at constant pressure, kJ/kg.K
fr	frequeny, Hz
g	gravitational acceleration, m/s^2
Gr	Grashof number
k	thermal conductivity, W/m.K
L	distance between cylinders
P	dimensionless pressure
p	pressure, Pa
Pr	Prandtl number, ν_f/α_f

Greek symbols

α	thermal diffusivity, m^2/s
β	volumetric coefficient of thermal expansion, K^{-1}
Ψ	dimensional stream function, m^2/s
ψ	dimensionless stream function
ΔT	temperature difference
λ	thermal conductivity of fluid, W/m·K
μ	dynamic viscosity, kg/m·s

Subscripts

c	cold
f	fluid

Abbreviations

Ra	Rayleigh number, $g\beta_f L^3\Delta T/(\nu_f\alpha_f)$
Re	Reynolds number, u_{in}·D/ν
Ri	Richardson number
T	temperature, K
Nu_s, $\overline{Nu_s}$	local and average Nusselt numbers on the cold surface
S_θ, S_ψ	entropy generation due to heat transfer and frictional irreversibilities
U,V	dimensionless velocity component in X- and Y-directions
u,v	velocity component in x- and y-directions (m/s)
X,Y	dimensionless coordinate in horizontal and vertical directions
x,y	Cartesian coordinates in horizontal and vertical directions, m
ν	kinematic viscosity, (μ /ρ)(Pa·s)
θ	dimensionless temperature, (T-Tc)/ΔT
ρ	density, kg/m^3
h	hot
s	source surface
B	base heat source
EG	entropy generation
v	vertical heat source

efforts to diversify the energy sources, currently 80% of energy demands are still met by fossil fuels [4]. The non-renewability and cost instability of petroleum-based fuels inspire researchers to develop novel approaches. One of the approaches is to enhance the efficiency of the heat transfer systems by evaluating the entropy generation (EG) that plays an important role not only in thermodynamics and heat transfer but also in fluid dynamics since the entropy concept and its generation are explained by the second law of thermodynamics. It is also a fact that there is friction between the fluid layers as they move, therefore, entropy is generated during their motion [5]. Furthermore, dissipative forces, mixing process, heat transfer, viscous forces, unrestrained expansion, and contraction, may cause EG.

The second law of thermodynamics deals with the quantity of energy produced in any process. Although the energy is conserved its quality may be degraded and the reduction in its quality is measured by EG. As the EG increases both the quantity and quality of the energy generated in a process reduce [6]. During the conversion of energy to something useful, energy is lost, hence, the performance of the systems or the devices used to convert energy decreases. It can be expressed that energy lost is directly proportional to EG. Hence, the amount of available energy decreases when the entropy is generated in a system. Therefore, minimizing the EG and increasing the heat transfer were the main goals of most studies performed in the past.

The entropy generation has been investigated by several researchers who mainly studied heat transfer in an enclosure. Deploying a rotating cylinder in an enclosure, Fu *et al.* [7] investigated how natural convection can be increased by rotation. It was found that the contribution of the rotating cylinder to natural convection depends upon the direction of the rotation of the cylinder. For their case, the rotation in the counter-clockwise direction contributed more to heat transfer. EG in a square enclosure that partly heated from a vertical wall was studied numerically by Erbay *et al.* [8]. They mainly focused on the effects of Prandtl (Pr) and Rayleigh (Ra) numbers on the EG during the transient laminar convection. It was reported that the maximum EG can be

experienced at higher Rayleigh number. Natural convection heat transfer between the nanofluid-filled circular enclosure and an elliptic cylinder was investigated numerically by Sheikholeslami *et al.* [9]. The influence of several parameters including *Ra*, inclination angle of the elliptic inner cylinder, and thermophysical properties of the nanofluid on the convection was examined. It was found that along with the *Ra* and nanoparticle volume fraction, the inclination angle of the inner elliptic cylinder increases the Nusselt number. Wang *et al.* [10] considered a rotating cylinder in a triangular enclosure to indicate the effects of rotating velocity, volume fraction of the used nanofluid, radius of the cylinder, and Rayleigh number. As reported previously, the direction of the rotation of the cylinder was found as one of the most important parameters of the thermal performance of the enclosure. A direct relationship between the Rayleigh and Nusselt numbers was also noted. Mixed convection along with the EG in a two-dimensional wavy-walled enclosure containing a rotating cylinder was investigated by the Galerkin method [11]. The combined effects of Rayleigh number, the number of oscillations, angular rotational velocity, and heat source length were investigated. It was emphasized that one can control the flow by changing the rotation velocity of the cylinder, and the Bejan number is the maximum for the case where the inner cylinder is almost stationary. Being different from the past studies by utilizing a trapezoidal enclosure, Yazdani *et al.* [12] considered natural convection heat transfer and its associated EG for the flow of a Non-Newtonian fluid through the porous media. Several parameters including the power-law index, the inclination angle of the side walls, and Darcy and Rayleigh numbers were examined as the controlling parameters for the flow. They concluded that there is a direct proportion between the side wall angle and EG and heat transfer. When the Darcy and Rayleigh numbers increase, the Bejan number declines whereas the frictional irreversibility in total irreversibility rises. Similar results were then reported by Dutta *et al.* [13] for a rhombic enclosure. Their interest in the phase shift angle revealed that the minimum EG for any value of Ra and Darcy numbers is obtained for a phase shift angle of $\pi/4$ and maximum for $3\pi/4$.

The studies on heat transfer exhibit that vibration and sound can also be used for the enhancement and control of heat transfer because any thermal device in operation deals with the vibration more or less, and such vibration may be used as a controlling parameter. Several innovative techniques such as rotating a solid body exposed to fluid at a different temperature, using a magnetic field and nanofluids, and enabling the vibration to enhance heat transfer have been reported so far. Among them, thermal vibrational convection are considered the least known but effective tool for controlling thermal convection. Most of the early investigations were generally experimental due to the lack of improved numerical techniques and unsufficient computational resources. Such experimental studies reported that the convection heat transfer coefficient and consequently the rate of heat transfer can be increased in general in the range of 30–300% by increasing the vibration frequency and amplitude of the vibrating cylinder, however, the local heat transfer rate does not increase in every part of the cylinder [14–18]. Interferometer studies also make it clear that the boundary layer becomes very complex and several transitions may be observed as the vibration intensity increases. However, at lower vibration intensity, it is similar to that of forced convection. When the vibration frequency of the cylinder is close to the natural shedding frequency of the flow heat transfer is maximum [19]. Although there are several experimental studies in the related literature the numerical studies are still rare. Some of them are referred to below.

Fu and Shieh [20] investigated convection within a two-dimensional square enclosure induced by gravity and vibration simultaneously. The effects of vertical vibration frequency on the convection heat transfer were mainly studied. It was reported that thermal convection can be divided into several regions and when the Rayleigh number is high, the gravitational thermal convection is dominant and surpasses the vibration effect on the heat transfer. However, in the low Rayleigh number, the vibration thermal convection dominates the heat transfer. Fuh and Shieh [21] studied the effects of high vibrating frequencies between 500 Hz and 5000 Hz on the transient

heat transfer by convection in an enclosure numerically. It was shown that increasing the vibration frequency reduces the time required for the transient process. Investigating the variations in frequency, amplitude, and Rayleigh number on natural convection from a heated source on a vertical plate, Fu and Huang [22] revealed that natural convection from the plate is smaller than that of the stationary state for the same Rayleigh number when frequency and amplitude change. Further, they concluded that when the frequency is higher than the critical one, increasing the amplitude and frequency enhance the heat transfer rate. In a two-dimensional numerical model, Xie and Zhang [23] considered four closely located cylinders vibrating in the vertical direction in a rectangular domain heated from the bottom. They showed that the thermal-hydraulic performance increases with vibrating frequency, however, decreases with increase in Reynolds number. Similarly to previous researchers, a direct relationship between the vibration frequency and heat transfer coefficient was reported. Using a vibrating concentric vertical cylinder at various vibration frequencies, Al-azzawi *et al.* [24] reported that the local heat transfer coefficient increases by heat input but declines with the axial distance to the cylinder. They revealed also that the local Nusselt number enhances along the cylinder axis from bottom to top. Kozlov *et al.* [25] experimentally investigated thermal vibrational convection in horizontal layers that were subjected to circular translational oscillations in the horizontal plane under the conditions of high negative Rayleigh numbers. It was discovered that the vibro-convective cells, which emerge in a threshold fashion upon reaching the threshold value of the vibration parameter, are distinguished by a considerable heterogeneity of sizes in different directions, disregarding the favored direction of translational vibration.

As aforementioned, most of the studies performed in the past dealt with heat transfer in enclosures. As a combination of natural and forced convection, the mixed convection heat transfer in enclosures has received much attention because of its practical importance in electronics and industrial processes such as cooling of electronic devices, nuclear reactors, chemical processes, lubricating grooves, coating, float glass manufacturing, and solidification processes [26–28]. Therefore, in the present article, heat transfer by mixed convection and EG of water flowing through a vented square cavity including vibrating cylinders are investigated numerically. The study is restricted only to mixed convection and heat transfer by conduction because compared to other mechanisms of heat transfer mixed convection is less investigated before. To the best of the authors' knowledge, although there are lots of studies dealing with EG, natural convection, and vibration in an enclosure, effects of the existence and vibration of multiple cylinders in an enclosure have not been reported so far. On this basis, the influence of vibration amplitude, frequency, and direction on the EG and heat transfer performance is investigated numerically on two-dimensional cases. This research aims to provide scientific responses to the following research questions.

- Can the presence of vibrating cylinders in the square vented enclosure enhance the overall heat transfer performance and affect the entropy generation compared to the case without cylinders, and if so, to what extent?
- What are the mechanisms underlying the changes in heat transfer and entropy generation behaviors of water inside the square vented enclosure with vibrating cylinders, and how do these mechanisms differ between horizontal and vertical cylinder orientations?

2. Computational details

2.1. Definition of problem

The flow of water past vibrating four cylinders in vertical and horizontal directions inside a square vented cavity is taken into account. The water with temperature T_i and freestream velocity

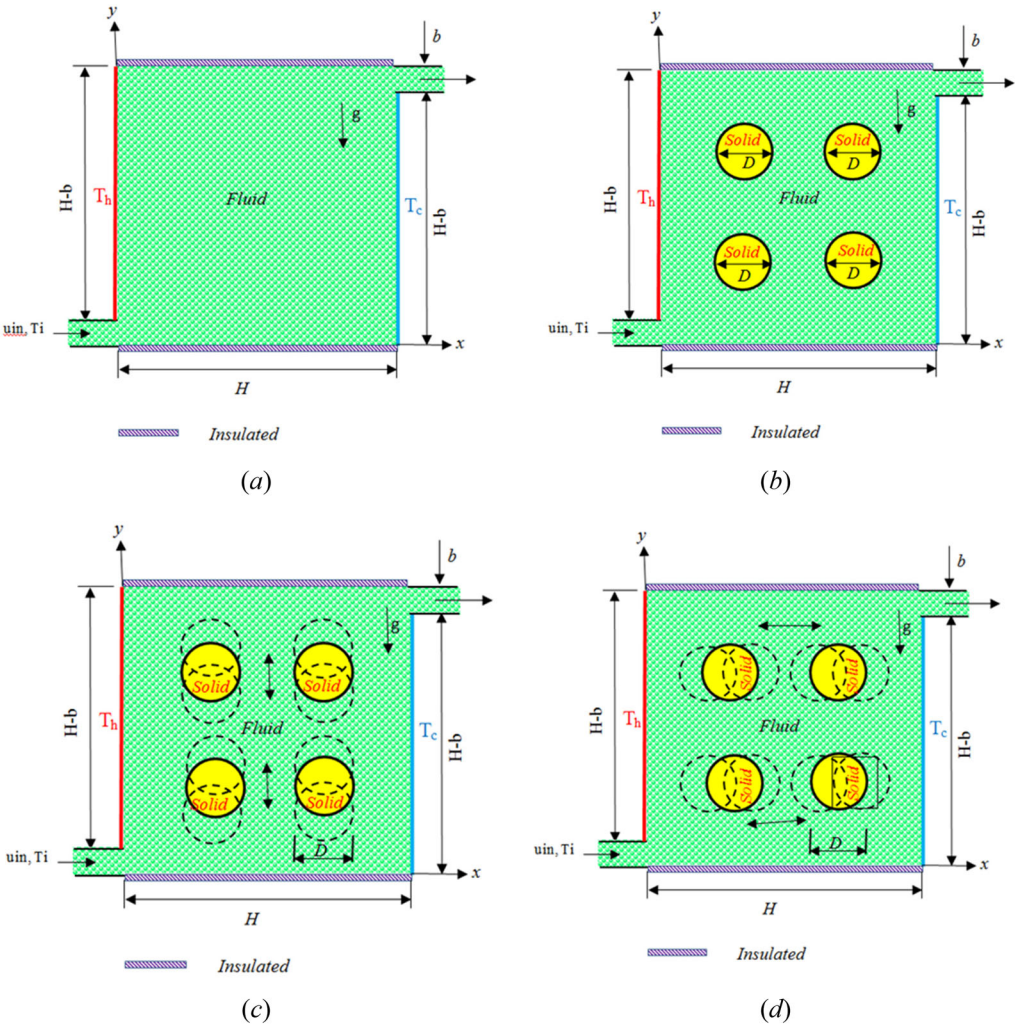

Figure 1. Sketch of the problem, (*a*) Case 1-enclsoure only, (b) Case 2-enclosure with fixed cylinders, (*c*) Case 3-enclosure with vibrating cylinders in *y*-direction, and (*d*) Case 4-enclosure with vibrating cylinders in *x*-direction.

u_i enters the cavity from a small inlet located at the bottom-left wall of the enclosure and leaves it from the top-right outlet. The left and right vertical walls of the enclosure are kept hot (T_h) and cold (T_c), respectively, while the top and bottom walls are insulated. The origin of the Cartesian coordinate system is located at the intersection of the left and bottom walls of the enclosure. As shown in Figure 1, four different cases are investigated. In the first case, there is not any cylinder in the enclosure (Case 1), while in the second case, four cylinders are fixed in the enclosure, that is, they do not vibrate in any direction. In the subsequent cases, the cylinders simultaneously vibrate in vertical direction (Case 3) and horizontal directions (Case 4), respectively. Therefore, as stated in Figure 1, each case are named as Case 1-Enclsoure only, Case 2-Enclosure with fixed cylinders, Case 3-Enclosure with vibrating cylinders in *y*-direction, and Case 4- Enclosure with vibrating cylinders in *x*-direction. The cylinders with diameter D are located separately with a distance L between them. The water flows over the cylinders under the influence of the gravitational acceleration $\overrightarrow{g}$. The square enclosure with length of H has one inlet and one outlet with the width of b.

2.2. Governing equations and boundary conditions

The three-dimensional flow over cylinder is complex and computationally expensive, hence, if the cylinder is long enough to prevent end effects the flow over cylinder can be predicted as two-dimensional. Such simplification reduces the complexity of the problem and enables researchers to concentrate on other parameters [29]. The governing equations of two-dimensional and unsteady flow past vibrating cylinders are continuity (Eq. (1)), momentum (Eqs. (2) and (3)), and energy (Eq. (4)) equations [30]. It was reported that the flow past a cylinder was classified as sub-critical when Reynolds number is between 10^3-2×10^5 [31, 32]. Therefore, the flow is assumed to be laminar in the present study. The working fluid (water) is assumed to be Newtonian and satisfies the Boussinesq approximation where density changes linearly with the temperature in the buoyancy term in the momentum equation. All other fluid properties are taken constant.

$$\frac{\partial u}{\partial x} + \frac{\partial v}{\partial y} = 0 \tag{1}$$

$$\rho\left(\frac{\partial u}{\partial t} + u\frac{\partial u}{\partial x} + v\frac{\partial u}{\partial y}\right) = -\frac{\partial p}{\partial x} + \mu\left(\frac{\partial^2 u}{\partial x^2} + \frac{\partial^2 u}{\partial y^2}\right) \tag{2}$$

$$\rho\left(\frac{\partial v}{\partial t} + u\frac{\partial v}{\partial x} + v\frac{\partial v}{\partial y}\right) = -\frac{\partial p}{\partial y} + \mu\left(\frac{\partial^2 v}{\partial x^2} + \frac{\partial^2 v}{\partial y^2}\right) + \rho\vec{g}\beta(T - T_c) \tag{3}$$

$$\rho C_p\left(\frac{\partial T}{\partial t} + u\frac{\partial T}{\partial x} + v\frac{\partial T}{\partial y}\right) = \lambda\left(\frac{\partial^2 T}{\partial x^2} + \frac{\partial^2 T}{\partial y^2}\right) \tag{4}$$

The diameter of the cylinder (D), inlet velocity (u_{in}) and pressure (p_0), hot (T_h) and cold (T_c) wall temperatures were used for nondimensionalization of the Eqs. (1)–(4) as shown below.

$$X = \frac{x}{D}, Y = \frac{y}{D}, \quad U = \frac{u}{u_{\text{in}}}, \quad V = \frac{v}{u_{\text{in}}}, \quad P = \frac{p - p_0}{\rho u_{\text{in}}^2}, \quad \theta = \frac{T - T_c}{T_h - T_c}, \quad \tau = \frac{t u_{\text{in}}}{D}$$

The normalized equations of continuity (Eq. (1)), momentum (Eqs. (2) and (3)), and energy (Eq. (4)) equations are given as follows, respectively.

$$\frac{\partial U}{\partial X} + \frac{\partial V}{\partial Y} = 0 \tag{5}$$

$$\frac{\partial u}{\partial \tau} + U\frac{\partial U}{\partial X} + V\frac{\partial U}{\partial Y} = -\frac{\partial P}{\partial X} + \frac{1}{Re}\left(\frac{\partial^2 U}{\partial X^2} + \frac{\partial^2 U}{\partial Y^2}\right) \tag{6}$$

$$\frac{\partial V}{\partial \tau} + U\frac{\partial V}{\partial X} + V\frac{\partial V}{\partial Y} = -\frac{\partial P}{\partial Y} + \frac{1}{Re}\left(\frac{\partial^2 V}{\partial X^2} + \frac{\partial^2 V}{\partial Y^2}\right) + Ri\theta \tag{7}$$

$$\frac{\partial T}{\partial \tau} + U\frac{\partial T}{\partial X} + V\frac{\partial T}{\partial Y} = \frac{1}{RePr}\left(\frac{\partial^2 \theta}{\partial X^2} + \frac{\partial^2 \theta}{\partial Y^2}\right) \tag{8}$$

where X, Y, U, V, P, θ, and τ are the dimensionless coordinates in x- and y-directions, velocity components in those directions, dimensionless pressure, temperature, and time. The nondimensional numbers called the Reynolds (Re), Grashof (Gr), Richardson (Ri), and Prandtl (Pr) numbers were obtained as given below:

$$Re = \frac{\rho u_{\text{in}} D}{\mu}, Gr = \frac{\vec{g}\beta(T - T_c)D^3}{\nu^2}, \quad Ri = \frac{Gr}{Re^2}, \quad Pr = \frac{\mu}{\rho\alpha}$$

The results of the study are given in terms of another nondimensional numbers such as the Nusselt number, ($Nu = \frac{hD}{\lambda}$) and the Bejan number (Be) [33]. The Bejan number is the ratio of heat transfer irreversibility (S_θ) to total irreversibility (S_{GEN}) that is due to heat transfer and fluid friction (S_ψ). It can be formulated as $Be = \frac{\int S_\theta dXdY}{\int S_{\mathrm{GEN}} dXdY}$. The S_{GEN} in dimensionless form is given in Eq. (9) as follows:

$$S_{\mathrm{GEN}} = \left(\frac{\partial\theta}{\partial X}\right)^2 + \left(\frac{\partial\theta}{\partial Y}\right)^2 + \emptyset^2\left\{2\left[\left(\frac{\partial U}{\partial X}\right)^2 + \left(\frac{\partial V}{\partial Y}\right)^2\right] + \left(\frac{\partial^2 U}{\partial Y^2} + \frac{\partial^2 V}{\partial X^2}\right)^2\right\} \tag{9}$$

Here, $S_{\mathrm{GEN}} = S_{\mathrm{gen}}\frac{T_0^2 D^2}{\lambda(\Delta T)^2}$ and $\emptyset = \frac{\mu_f T_0}{k_f}\left(\frac{\alpha_f}{D\Delta T}\right)^2$ where $\emptyset$ is the reversibility distribution rate. Irreversibility due to heat transfer (S_θ) and fluid friction (S_ψ) can be written as $S_\theta = \left(\frac{\partial\theta}{\partial X}\right)^2 + \left(\frac{\partial\theta}{\partial Y}\right)^2$ and $S_\psi = \emptyset^2\left\{2\left[\left(\frac{\partial U}{\partial X}\right)^2 + \left(\frac{\partial V}{\partial Y}\right)\right] + \left(\frac{\partial^2 U}{\partial Y^2} + \frac{\partial^2 V}{\partial X^2}\right)^2\right\}$, respectively. So, as aforementioned $S_{\mathrm{GEN}} = S_\theta + S_\psi$ and integrating this one over the computational domain provides the global entropy generation (GEG) as $\mathrm{GEG} = \int S_\theta dXdY + \int S_\psi dXdY$. Bejan number changes in the range of $0 < Be < 1$. The total EG is dominated by thermal irreversibilities when $Be > 0.5$ and by frictional irreversibilities when $Be < 0.5$. The contribution of these two factors are equal for the special case of $Be = 0.5$ as implied by Alsabery *et al.* [11].

The governing equations for two-dimensional heat transfer and laminar flow of water passed solid vibrating cylinders in an enclosure are solved on the finite element method with second-order approach [34]. Details on the grids generated by dividing the enclosure domain, grid independency study, initial and boundary conditions along with the validation process are given in the present section.

2.3. Grid independence study

Nonuniform unstructured triangular grid elements are generated as shown in Figure 2. More elements are concentrated near the walls and in the vicinity of the cylinders to capture the steep gradients of velocity and temperature. As the base grid, 2292 elements are generated first, and then, the number of grids is increased systemically for a mesh independence study.

Five different grid sizes are studied to ensure that the results are independent of the number of the grid elements. The Nusselt number obtained with each grid size is shown in Table 1. The difference in the Nusselt number obtained with each grid was calculated as proposed by Maougal and Bessaih [35].

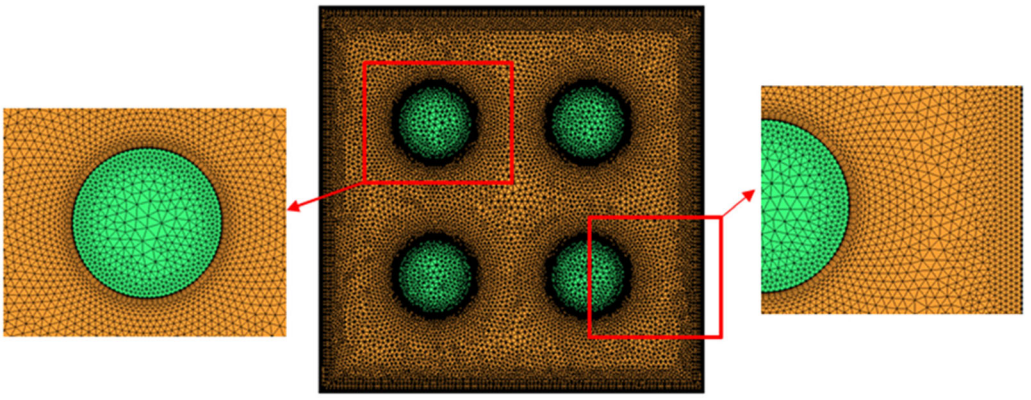

Figure 2. Mesh structure applied to the enclosure and the cylinders.

Table 1. Grid independent study, $Re = 150$, $Ri = 10$, $fr = 5$ Hz, $A = 0.1$L, Case 3.

Grid	Domain elements	Boundary elements	Time (sec)	Nu_{avg} (–)	Error (%)
G1	2992	190	3582	23.600	–
G2	3572	216	3620	23.400	0.85
G3	5044	260	3720	23.189	0.90
G4	14,744	742	4012	25.408	9.57
G5	25,940	792	4220	25.412	0.02

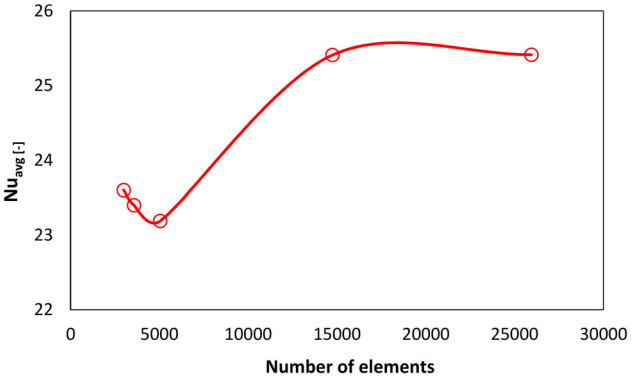

Figure 3. Change in the average Nusselt number with the number of domain elements.

$$\text{Error } (\%) = \left| \frac{N^2_{s(k,k)} - N^1_{s(k,k)}}{N^1_{s(k,k)}} \right| \tag{10}$$

where $N_{s(k,k)}$ is the previously calculated value of the average Nusselt number on the surface corresponding to the mesh size (k,k). Table 1 presents Nusselt number values for each chosen grid and the associated relative error (difference). This calculation is done for $Re = 150$, $Ri = 10$, $fr = 5$ (1/s), $A = 0.1$L for Case 3.

The outcomes of the grid independence study reveal that the relative error obtained with grid 5 (G5) is the lowest, however, G4 provides relatively faster solution when computational time is considered. Based on the good compromise between the accuracy of the calculations and the computation time, all remaining calculations are performed with grid 4 (G4). The trend in the change of Nusselt number with increasing mesh elements can be seen in Figure 3. Since using more elements changes the Nusselt number 0.02% only the G4 was used during the numerical calculations.

The governing equations shown in previous section are solved iteratively until the solution is converged. It is assumed that the iterative procedure is converged when it satisfies the following convergence criterion.

$$\left| \frac{\varphi^{n+1} - \varphi^n}{\varphi^{n+1}} \right| \leq 10^{-5} \tag{11}$$

where φ and n show any variables and iteration level, respectively.

2.4. Validation of the model

The validity of the computational model developed for the solution of the problem under consideration is presented in this section. Due to the lack of a similar experimental or numerical study, validation of the present study is performed by considering the cases investigated by Chamkha *et al.* [36] and Nosonov and Sheremet [27]. As shown in Figures 4 and 5, the results are

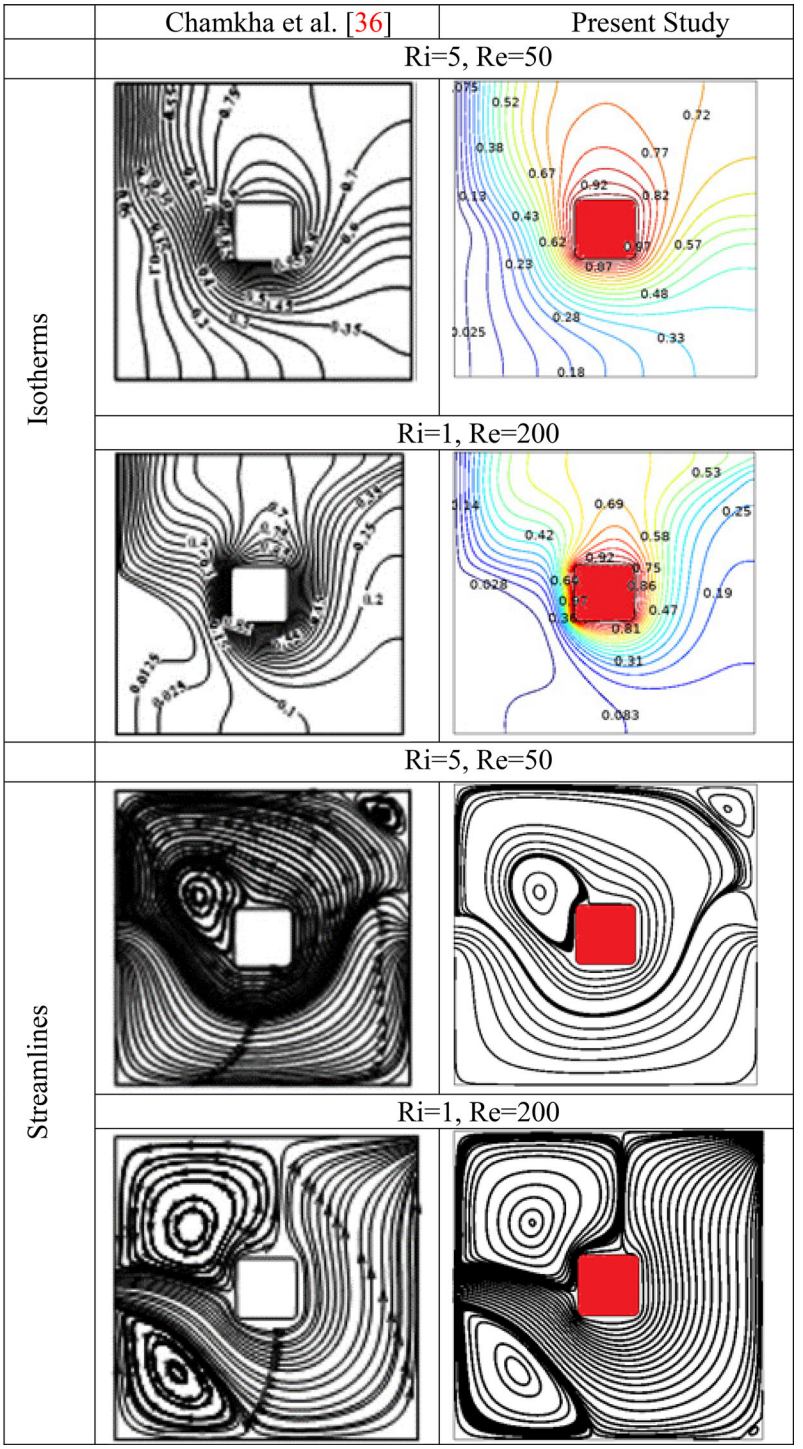

Figure 4. Comparison of isotherms (top) and streamlines (bottom) with Chamkha *et al.* [36], $Pr = 0.71$.

comparatively presented in terms of streamlines and isotherms for various Reynolds and Richardson numbers. Figure 4 illustrates streamlines and isotherms reported by Chamkha *et al.* [36] for mixed convection from a heated square cylinder in a cavity with two small openings.

The cavity was filled with fluid at $Pr = 0.71$. The top, right, and bottom walls of the cavity were adiabatic while the left wall was taken at a relatively lower temperature than that of the solid cylinder.

An additional comparison is made with results provided by Nosonov and Sheremet [27] for mixed convection in an open cavity having local heaters of different sizes, (Figure 5). The location of the heater was changed systematically to reveal the cooling effectiveness of the model. The comparisons are made for two different Richardson numbers, $Ri = 0.1$ and 1 at $Re = 100$. As shown in Figures 4 and 5, both the isotherms and streamlines obtained at various Richardson and Reynolds numbers are in good agreement with those reported by Chamkha *et al.* [36] and Nosonov and Sheremet [27].

3. Results and discussion

The present work is devoted to disclose the effects of thermo-convective parameters on heat transfer and entropy generation of water flowing in a vented enclosure that contains four vibrating cylinders. The change in streamlines and isotherms for each case where the enclosure does not contain any cylinder (Case 1), the cylinders are fixed in the enclosure (Case 2), the cylinders vibrate in the vertical direction (Case 3), and finally, the cylinders vibrate in the horizontal direction (Case 4) are shown in Figure 6 for three Reynolds numbers ($Re = 50$, 100, and 150).

3.1. Effects of Reynolds and Richardson numbers

The fluid enters the enclosure from the inlet at the bottom-left side of the enclosure and leaves it from the top-right exit. The left wall is hotter than the right wall of the enclosure. Under these conditions, it is seen that a large recirculation region occurs at $Re = 50$ when the enclosure is empty (Case 1) and it grows in size as the Reynolds number increases as reported by several researchers [37–39]. This is due to the fact that at high Reynolds number, the flow is dominated by inertial forces that cause larger recirculation region. A similar formation can be observed when the enclosure contains four fixed solid cylinders (Case 2). As Reynolds number increases the flow region is distorted and small-scale recirculation regions around the cylinders are formed. Regardless of the Reynolds number, the flow field is divided into columns that are almost symmetric to the vertical direction when the cylinders vibrate with $fr = 5$ Hz in the vertical direction (Case 3). The amplitude of the cylinders in the vertical direction, in this case, is $A = 0.05$L where L is the distance between the centers of the cylinders. With the same frequency and amplitude, the cylinders vibrate in the horizontal direction in Case 4 where the vibration of cylinders in the horizontal direction leads to a similar formation in the horizontal direction.

Implying the significance of the buoyancy effects on the fluid-structure with respect to shear forces ($Ri = \frac{Gr}{Re^2}$), the influence of the Richardson number can be seen by comparing Figures 6 and 7 where it is observed that when the Richardson increases the recirculation regions formed at the lower Richardson number in Figure 6 stretch toward the vertical walls of the enclosure and the velocity of the fluid increases while it flows from the inlet to the outlet in Case 1. In Case 2 where the enclosure contains the cylinders, it is seen that some additional recirculation regions are formed and those exist at low Richardson numbers grow in size. This is in consistent with previous studies [40, 41]. Basically, except for the formation of smaller recirculation regions formed beneath the top wall of the enclosure, the flowfield seems to be the least affected when the cylinder makes a translational vibration in the vertical direction (Case 3). In Case 4 where the cylinders vibrate in the horizontal direction, the flowfield is almost the same as those for $Re = 5$.

The change in isothermal lines with Reynolds number is depicted in Figures 8 and 9 for the Richardson numbers, $Ri = 5$ and 100, respectively. At both Richardson numbers, it is observed that as the Reynolds number is boosted, the heat is transferred more effectively by convection from the heating wall to the adiabatic top wall and exits the enclosure since the maximum

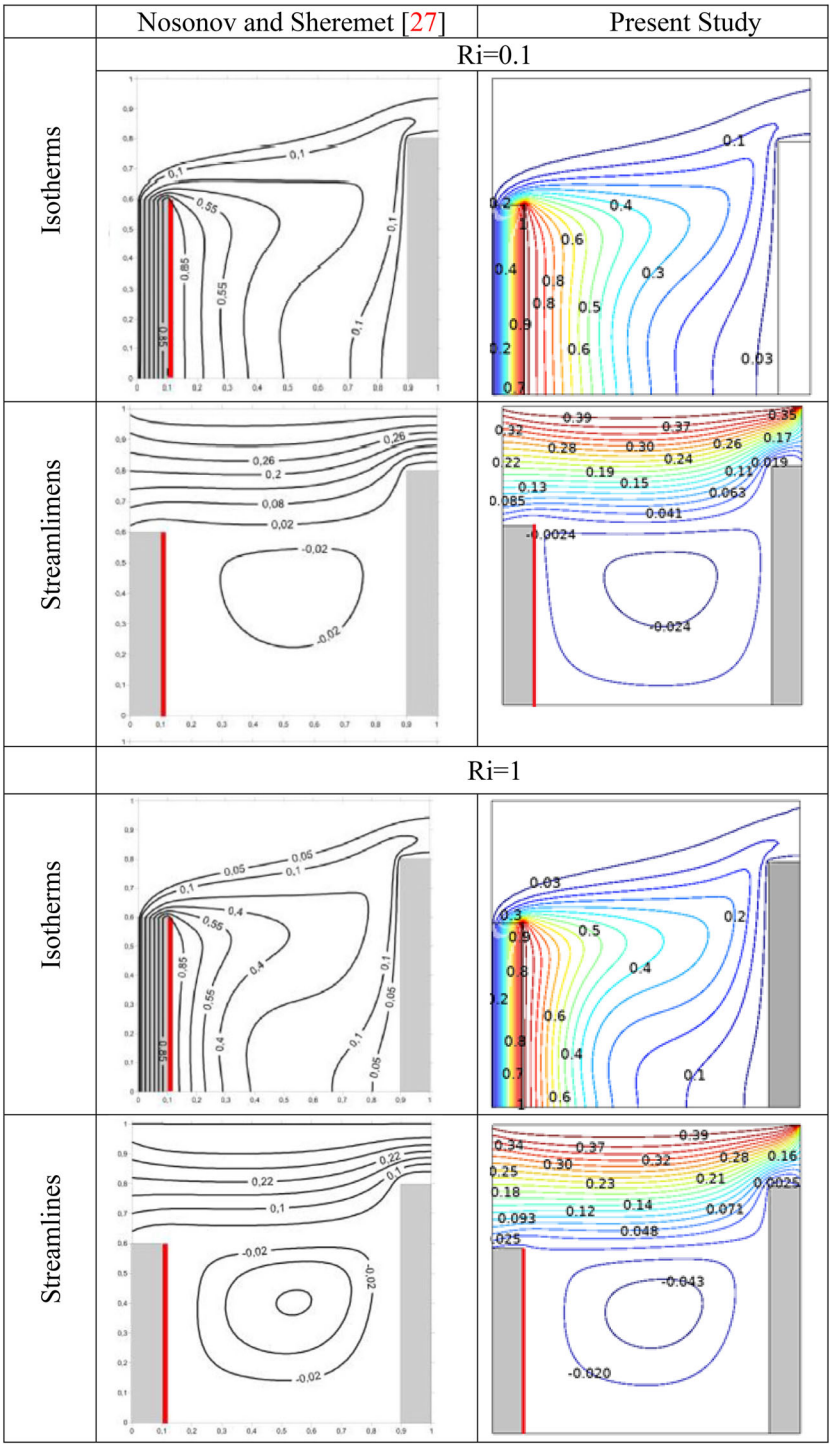

Figure 5. Comparison of isotherms (left) and streamlines (right) with Nosonov and Sheremet [27], $Re = 100$.

temperature contours are transported to these regions as the fluid moves to the exit of the enclosure. Likewise, as the Richardson number increases the isotherms change their directions and move parallel to the bottom wall specifically at the center of the enclosure indicating

improvement in the convection heat transfer. The cylinders, behaving as obstacles to the oncoming flow make the temperature field more compact. As they vibrate the uniformity of the isotherms in the entire flowfield is distorted from the shapes corresponding to diffusion heat transfer. When the cylinders vibrate in the horizontal direction, the thermal gradients become more clustered and the isotherms are denser accordingly in the left vertical and top walls as the Reynolds number increases.

Below figures show the change in isotherms with Reynolds number for $Ri = 100$ (Figure 9). Comparing with the isotherms presented for $Ri = 5$ in Figure 8, it can be concluded that the rise in the Richardson number leads the isothermal lines to be parallel to the bottom or top wall at all cases. In addition, the vibration of the cylinders in the vertical direction (Case 3) forces the isothermal lines to move upward and increases heat transfer specifically near the adiabatic top

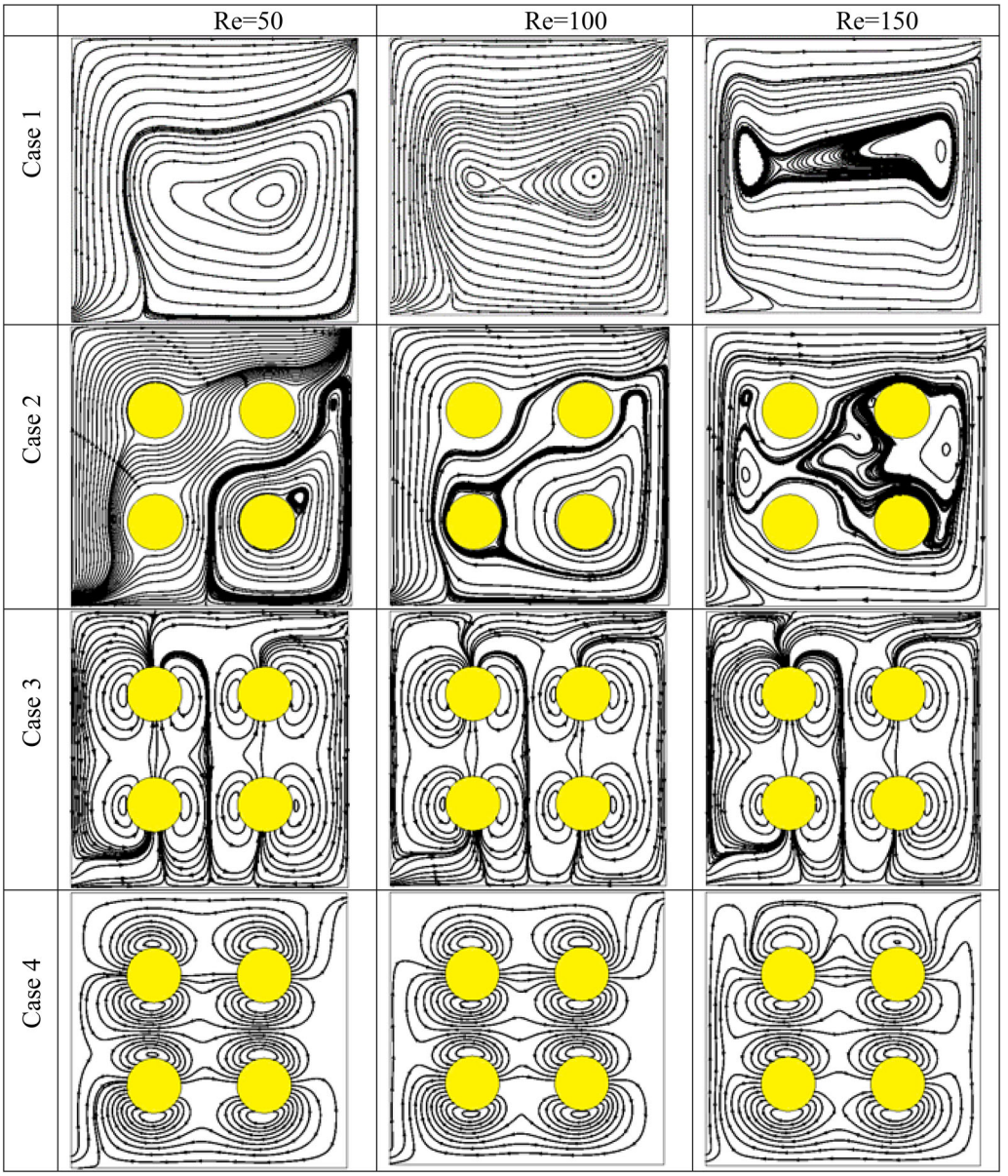

Figure 6. Comparison of fluid structure at various Reynolds numbers at $Ri = 5$ ($fr = 5$, $A = 0.05$L).

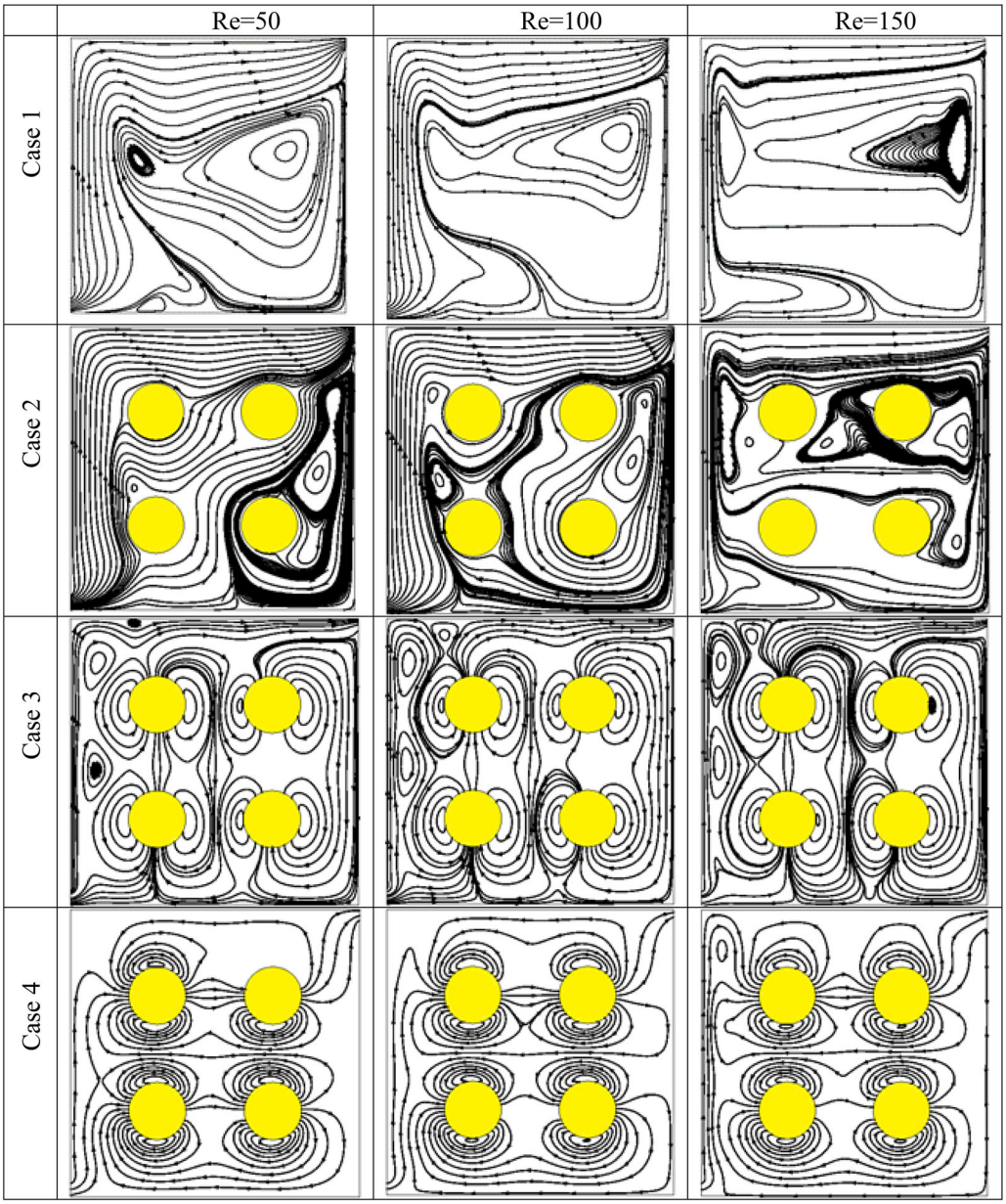

Figure 7. Comparison of fluid structure at various Reynolds number at $Ri = 100$, ($fr = 5$, $A = 0.05$L).

wall while the vibration of the cylinders in the horizontal direction (Case 4) at higher Richardson number ($Ri = 100$) causes the isothermal lines packed densely to the side vertical walls. In summary, any increment in both Reynolds and Richardson numbers contributes to convection heat transfer like the vibration of the cylinders either vertical or horizontal direction.

3.2. Effects of amplitude of the cylinders

It was reported that as the amplitude of the frequency increases, the convection heat transfer improves considerably [42]. Using a flexible fin in a cavity Ghalambaz *et al.* [43] shown that the Nusselt number increases with the enhances of the oscillating fin's amplitude as the interaction of

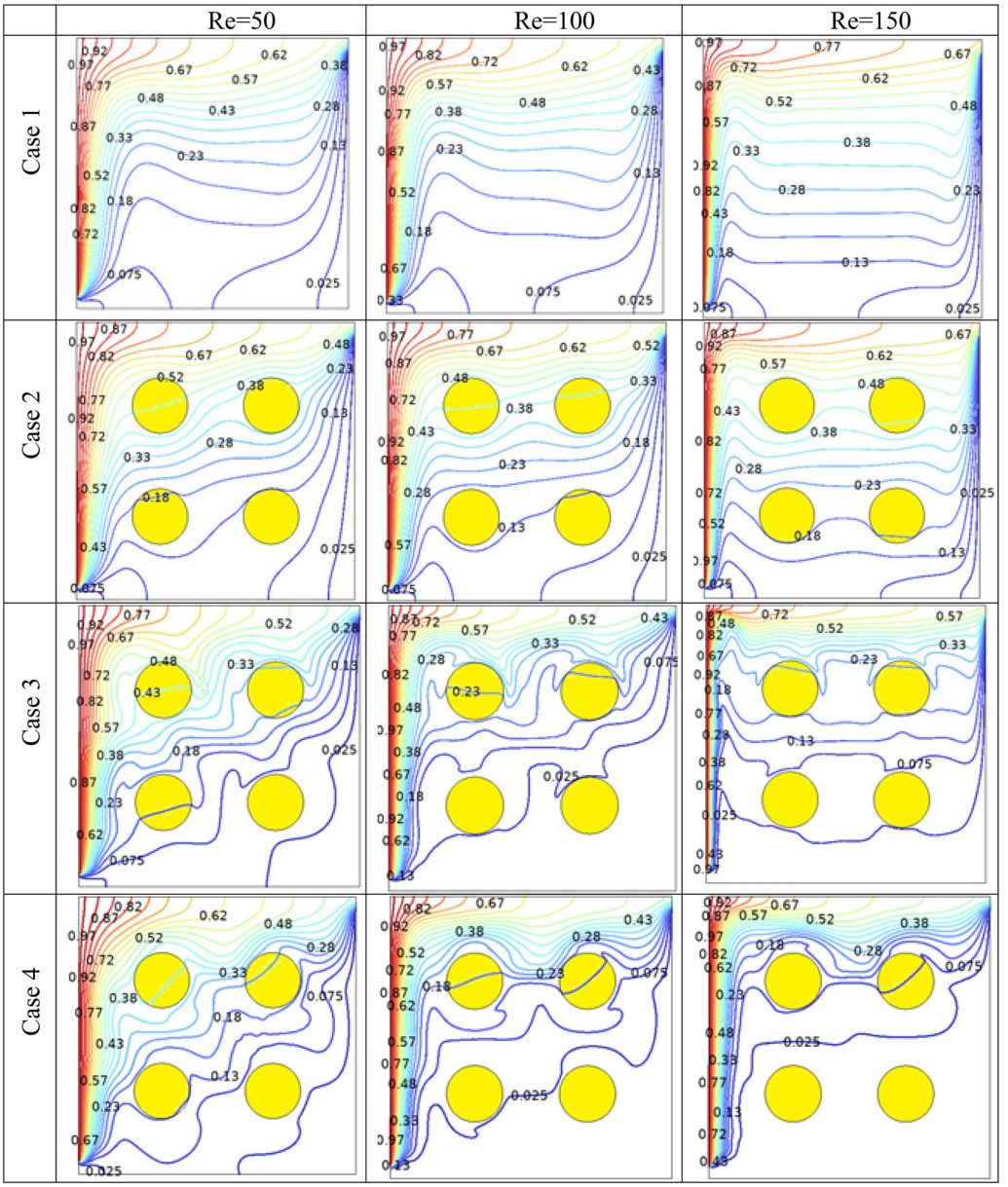

Figure 8. The change of isothermal field with Reynolds numbers at $Ri = 5$, $fr = 5$, $A = 0.05$L.

the cold fluid and hot wall increases with larger amplitude. The effects of the amplitude (A) on the flowfield and isothermal lines are shown in Figure 10 for the cases where the cylinder vibrates in vertical (Case 3) and horizontal (Case 4) directions for $A = 0.025$L, 0.05L, and 0.1L. The direction of vibration of the cylinders specifies the type of flowfield in each case. For example, when the cylinders vibrate in the vertical direction the flowfield is divided basically into two flow regions relative to the vertical axis passing through the center of the enclosure while it is divided into two flow regions relative to the horizontal axis passing through the center of the enclosure when the cylinders vibrate in the horizontal direction, as well. As the Reynolds number rises the vibration of the cylinders in the vertical direction complicates the isothermal lines around the cylinders, however, this is not the case for the vibration in the horizontal direction.

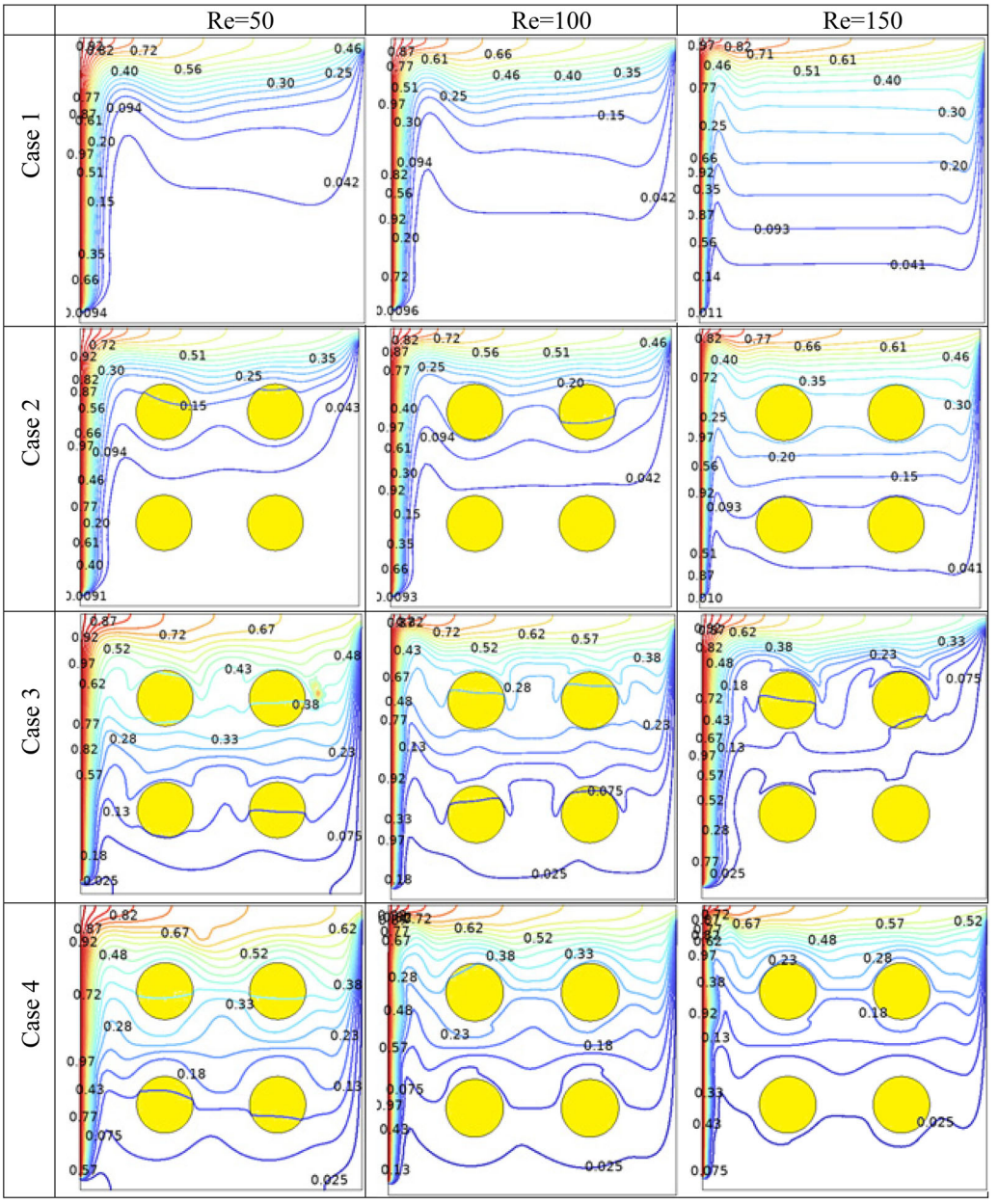

Figure 9. Change of isothermal field with Reynolds number at $Ri = 100$, $fr = 5$, $A = 0.05L$.

The time history of the flowfield is illustrated in Figure 11 for Case 4 at $Re = 150$ and $Ri = 100$. These figures show embedded streamlines to the contours of the current intensity. The changes are depicted from the nondimensional time $\tau = 9.80$ to $\tau = 10$ with $\tau = 0.02$ increments. In Case 4, the cylinders vibrate in the horizontal direction at frequency $fr = 5$ with amplitude $A = 0.1L$. The contours reveal the vibration of the cylinder with time. The cylinders in motion toward to left wall squeeze the flow in the region between the left wall and the cylinders due to reduced area in that region and cause strong vortices. After some time, when the cylinders vibrate in the opposite direction the vortices upstream of the cylinders diminish and the vortices compose downstream of the cylinders.

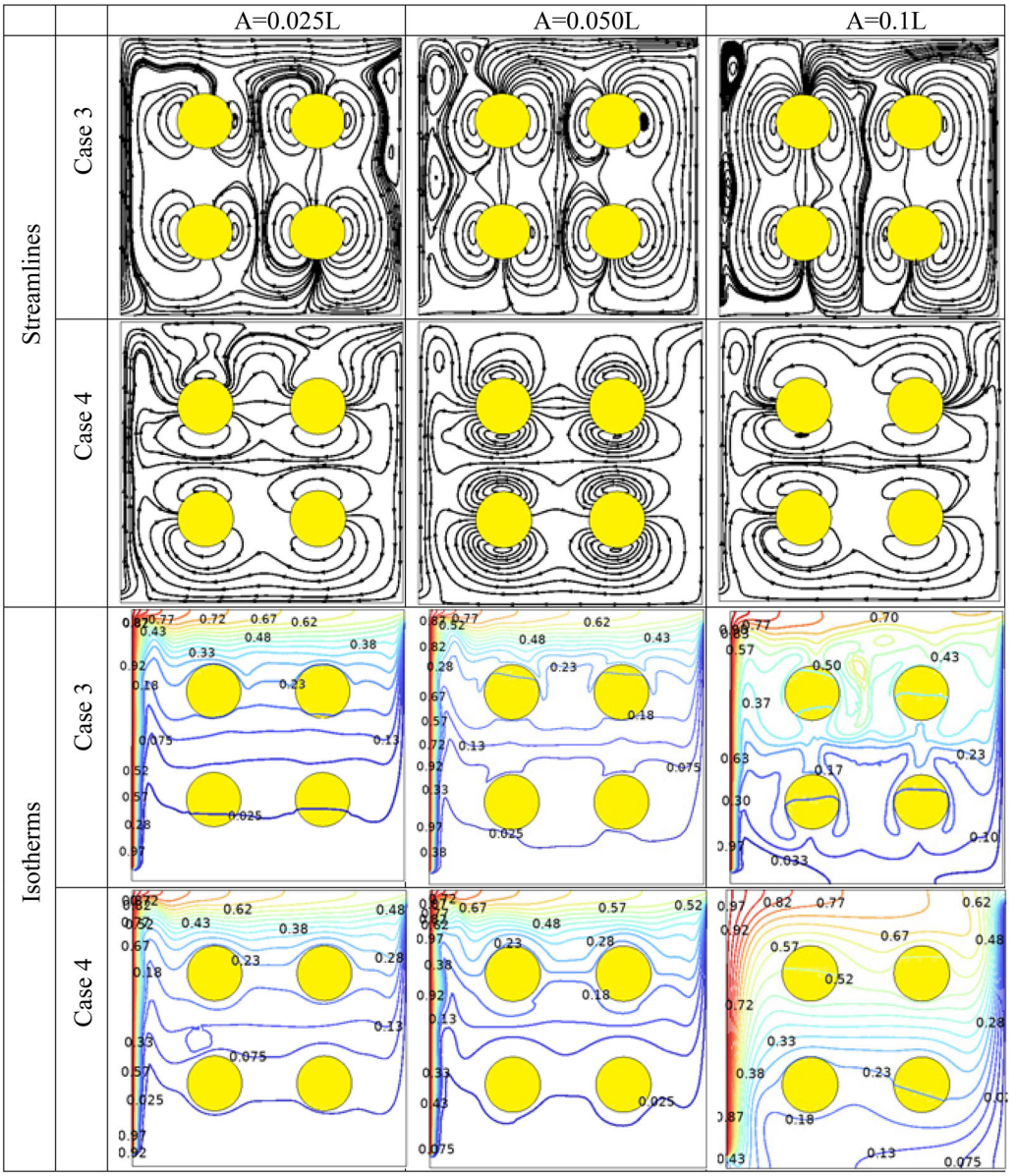

Figure 10. Comparison between Cases 3 and 4 of streamlines and isotherms for different amplitudes at $Re = 150$, $Ri = 100$, $fr = 5$.

3.3. Entropy generation

The heat transfer component of the entropy generation (EG) is illustrated in Figure 12 for various Reynolds numbers and the cases investigated in the article. As Reynolds number increases, the maximum value of EG increases on the left heated wall regardless of the existence and even vibration of the cylinders. This is not surprising since friction occurs between the wall and moving fluid on the hot vertical wall [44]. The figures depict that the EG due to heat transfer is negligible at the center of the enclosure and adiabatic walls do not contribute to EG in terms of heat transfer. A similar conclusion was reported before by Soleimani *et al.* [45] for laminar natural convection in an enclosed cavity. The fixed cylinders that do not vibrate in any direction

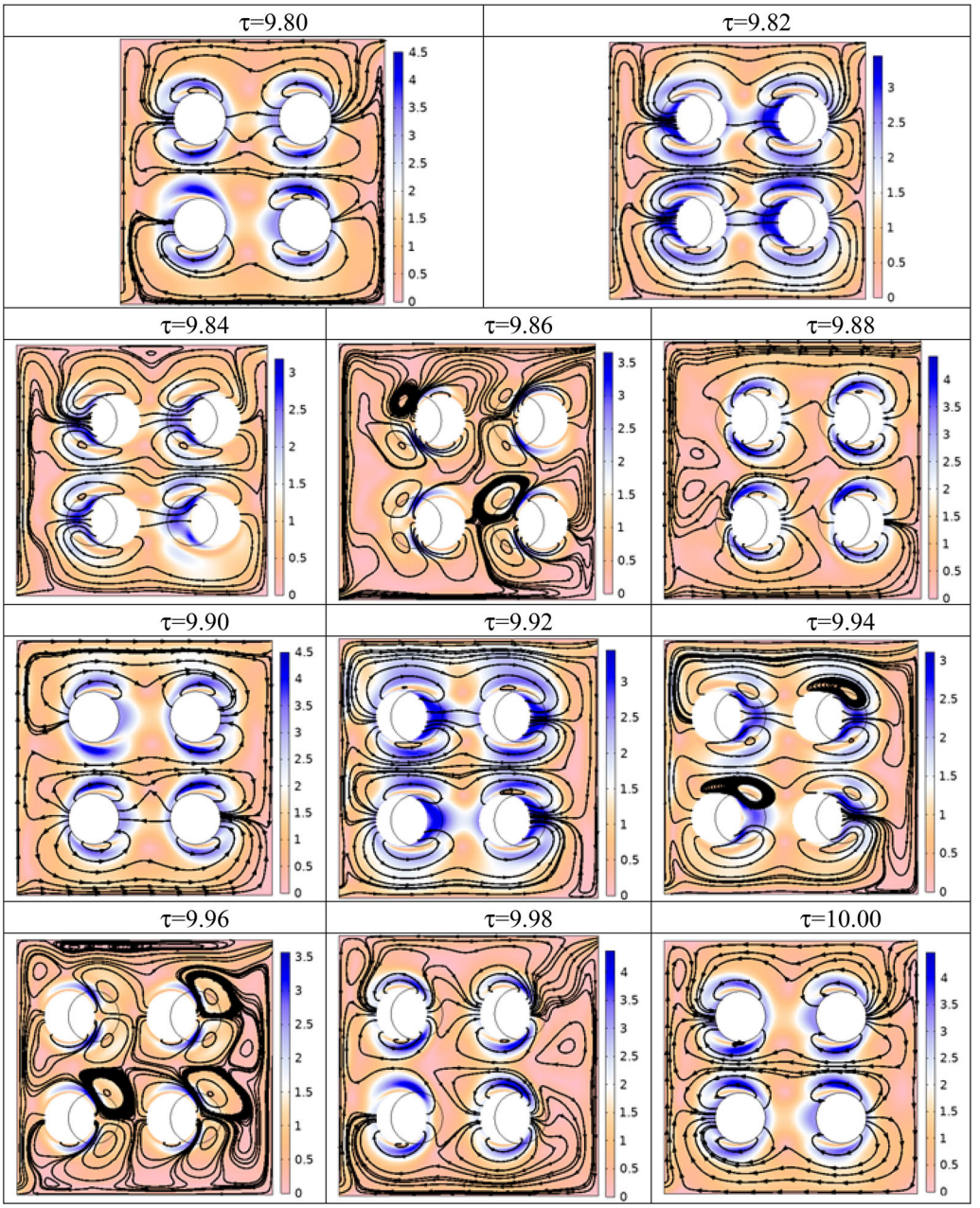

Figure 11. Change in flowfield with time (Case 4, $Re = 150$, $Ri = 100$, $A = 0.1L$, $fr = 5$).

contribute to decreasing the maximum value at the specified Reynolds number. When the cylinders vibrate in the vertical direction, they contribute to the maximum value by increasing EG due to heat transfer while it reduces for the case where cylinders vibrate in the horizontal direction.

The contour of the Bejan number which is a measure of the importance of thermal and frictional EG to the total EG is shown in Figure 13. The Bejan number is the lowest at the adiabatic top and bottom walls of the enclosure but maximum over the vertical walls (Case 1). The homogenous distribution of the Bejan number is distorted as the cylinders are placed in the flowfield. Relatively small Bejan numbers can be observed upstream and downstream of the cylinders due

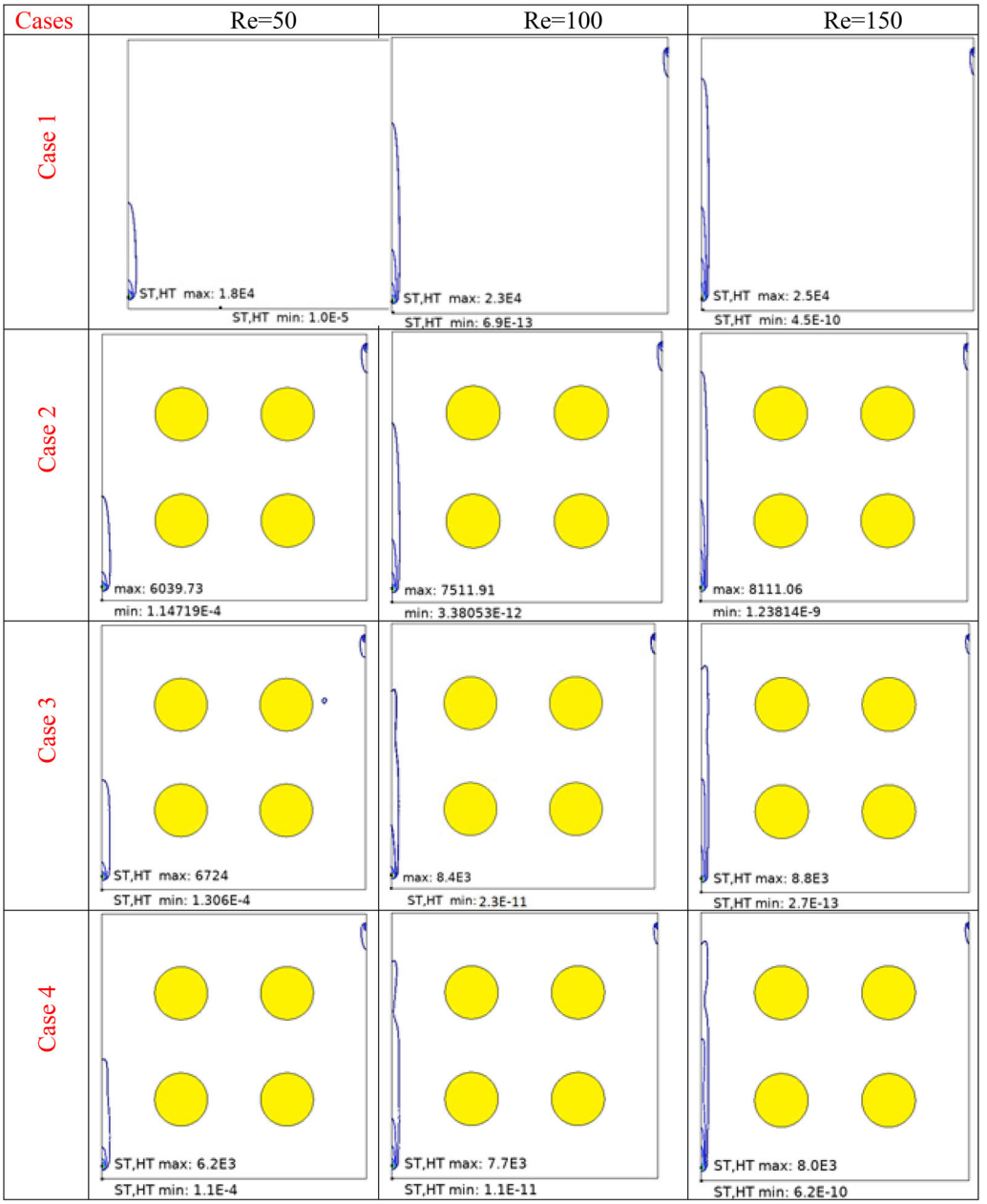

Figure 12. Comparison of the entropy generation at each case due to heat transfer for different Reynolds number at $Ri = 100$, $A = 0.1L$, $fr = 5$.

to the interaction of the flow with the fixed cylinders in Case 2. In the first two cases, it seems that the Reynolds number does not affect the Bejan number considerably. However, as the cylinders vibrate with a frequency of $fr = 5$ and amplitude $A = 0.1L$ in the last two cases the Bejan number changes and decreases around the cylinder due to the motion of the cylinders that enhances the irreversibility due to heat transfer in those regions. As reported by Zadeh *et al.* [46] for a similar case, the *Be* is identical to unity throughout the vertical walls.

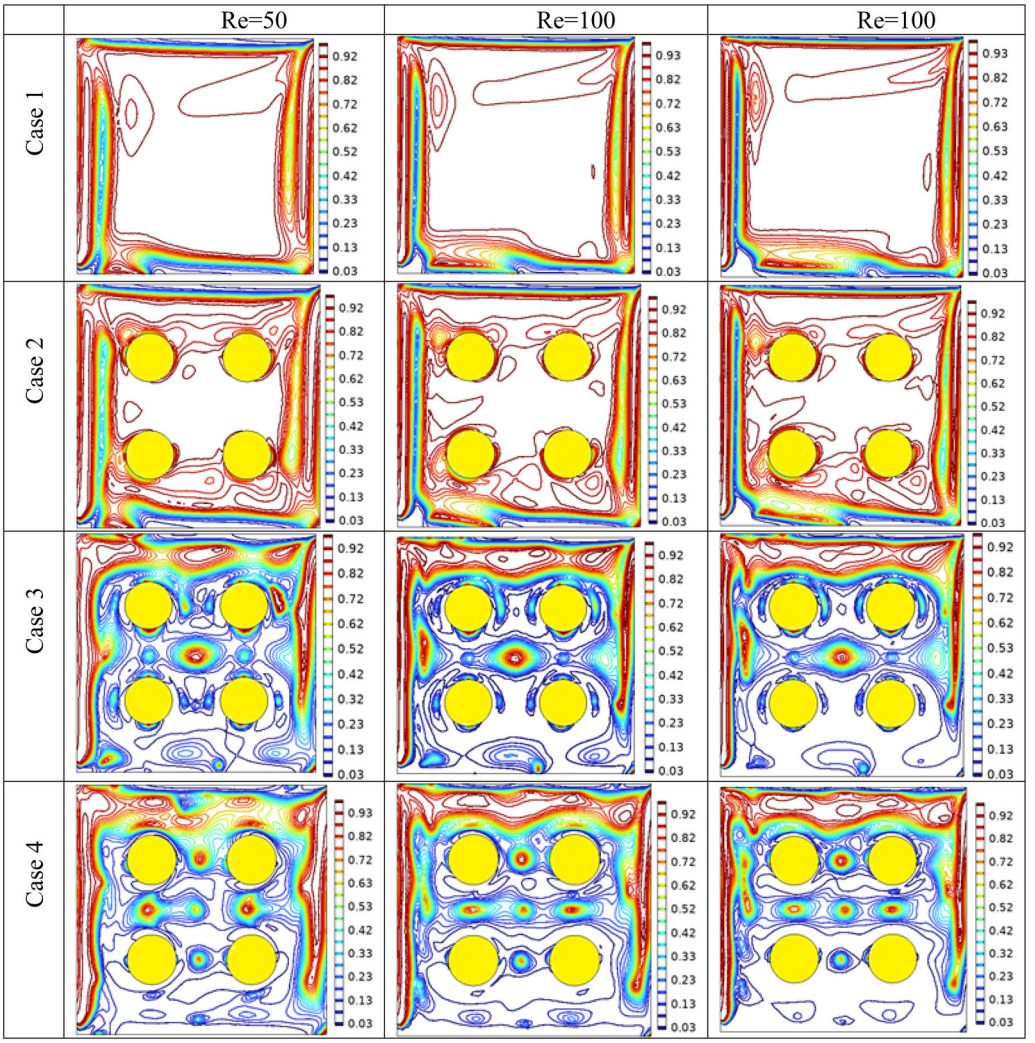

Figure 13. Comparison of the Bejan number for different cases and Reynolds numbers, ($Ri = 100$, $A = 0.1L$, $fr = 5$).

3.4. Variation in the Nusselt number

The trends in the Nusselt number along the heated left wall are displayed in Figure 14 for various Reynolds and Richardson numbers which characterize the flow type and serve as a measure of the effects of free convection concerning forced convection. At the same location on the heated wall, the largest Reynolds and the Richardson numbers provide maximum heat transfer while in contrast, the minimum heat transfer occurs at the lowest Reynolds and the Richardson numbers. The local Nusselt number distribution on the heated wall of the enclosure with and without cylinders is almost the same since the cylinders are fixed (Case 2) and relatively far from the left wall. However, when the cylinders vibrate in the vertical direction (Case 3) the Nusselt number fluctuates along the wall, making local the Nusselt number maximum due to the recirculation regions formed around the cylinders. Unlike the plots in Figures 13*a*–13*c* where the effects of the Reynolds and Richardson numbers are shown together, Figure 14*d* presents the effects of Richardson numbers only for $Re = 100$. Here, it can be shown that the heat transfer through natural convection increases as the Richardson number rises.

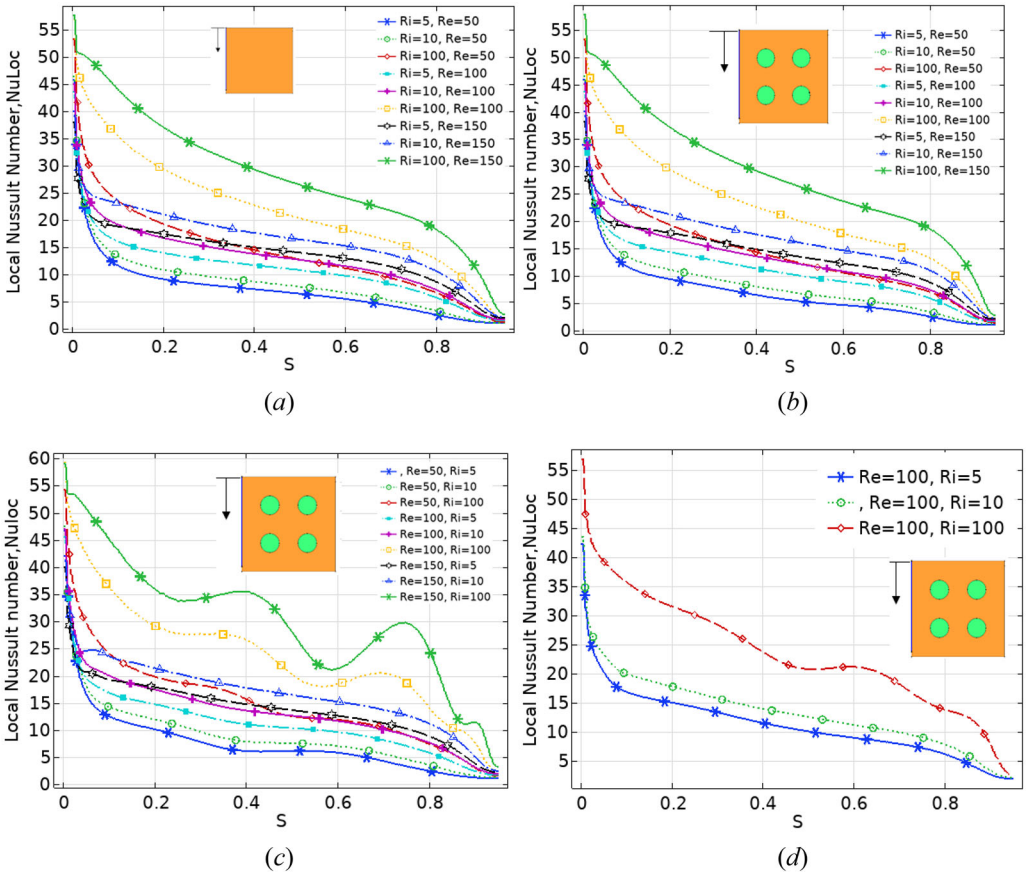

Figure 14. Local Nusselt number distribution along left heated wall for different Reynolds and the Richardson numbers at $A = 0.05L$, $fr = 5$, (*a*) Case 1, (*b*) Case 2, (*c*) Case 3, and (*d*) Case 4.

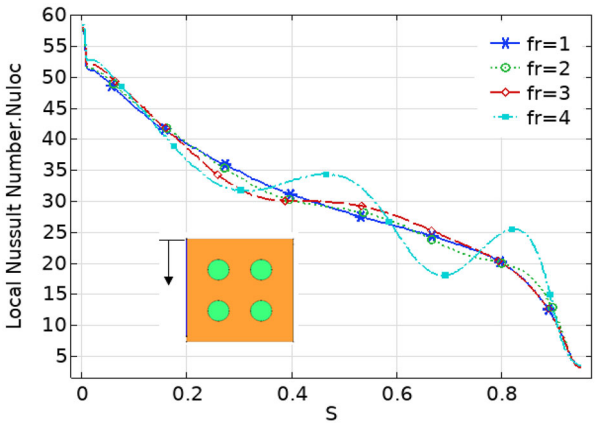

Figure 15. Local Nusselt number along left heated wall for different frequencies at $A = 0.05L$, $Re = 150$, $Ri = 100$, Case 4.

The influence of the vibration frequency on the heat transfer from the heated wall is shown in Figure 15 as the cylinders vibrate in the horizontal direction (Case 4). The local Nusselt number is the maximum at the lower end of the wall and the minimum at the intersection of the heated wall with the adiabatic top wall. Between these two ends, the heat transfer by convection

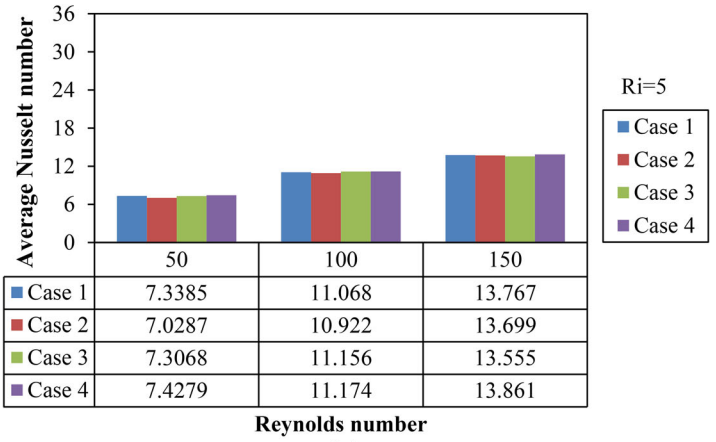

	50	100	150
Case 1	7.3385	11.068	13.767
Case 2	7.0287	10.922	13.699
Case 3	7.3068	11.156	13.555
Case 4	7.4279	11.174	13.861

Reynolds number

(*a*)

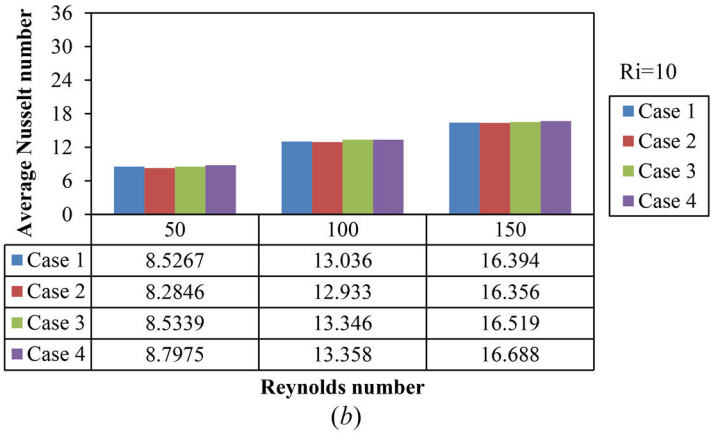

	50	100	150
Case 1	8.5267	13.036	16.394
Case 2	8.2846	12.933	16.356
Case 3	8.5339	13.346	16.519
Case 4	8.7975	13.358	16.688

Reynolds number

(*b*)

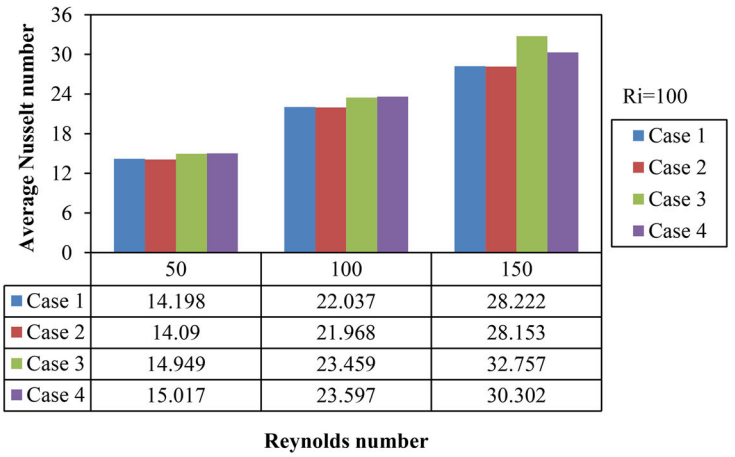

	50	100	150
Case 1	14.198	22.037	28.222
Case 2	14.09	21.968	28.153
Case 3	14.949	23.459	32.757
Case 4	15.017	23.597	30.302

Reynolds number

(*c*)

Figure 16. Average Nusselt numbers for various cases and Reynolds numbers (*a*) $Ri = 5$, (*b*) Ri = 10, (*c*) Ri = 100 ($A = 0.05$L, $fr = 5$).

decreases from $Nu_{loc} = 60$ to zero. Between $0 < s < 0.2$ where s is the length of the heated wall the magnitude of the local Nusselt is the same which indicates that the vibration frequency of the cylinders does not affect the convection heat transfer. However, as fluid moves upward heat

transfer is affected by the frequency of the vibrating cylinders. Frequency $fr = 4$ is prominent in terms of heat transfer on two points on the heated wall because there is two local maximum of Nusselt number exist.

Heat transfer performance of all cases considered in current study is compared in Figure 16 in terms of the average Nusselt number for three Reynolds ($Re = 50$, 100, and 150) and Richardson ($Ri = 5$, 10, and 100) numbers. It can be verified that the heat transfer by convection raises with increasing Reynolds number and as the Richardson number increases the average Nusselt number enhances with Reynolds number. The plots reveal that, with respect to enclosure without the cylinders (Case 1), the existence of the cylinders (Case 2), and vibration of them in vertical (Case 3), and then, in horizontal direction (Case 4) increases the heat transfer at any Richardson number. To quantify the observed increase in the average Nusselt number due to rising of Reynold number, it is realistic to adopt the slope linear regression through the data points presented by Animasaun *et al.* [47], adopted and found to be a useful technique for data exploration by Cao *et al.* [28] and Saleem *et al.* [48]. Therefore, the slope of linear regression across the data points was used as recommended [49]. For case 1, the average Nusselt number increases due to higher Reynold number at the rate of 0.064285. For the second case, the average Nusselt number increases due to higher Reynold number at the rate of 0.066761. In addition, for the third case, the average Nusselt number increases due to higher Reynold number at the lower rate of 0.062482. It is worth noticing in the fourth case that the average Nusselt number increases due to higher Reynold number at the rate of 0.064331.

When Richardson number increases to $Ri = 10$, the Nusselt number for each cases increases with higher rates according to linear regression method as follows; for case 1 the Nusselt number increases with Reynolds number at the rate of 0.078673 while for the Case 2, it increases with Reynolds number at the rate of 0.080714. The Nusselt number increases at the rate of 0.079851 and 0.078883 when Reynolds numbers increase to 100 and 150, respectively, at $Ri = 10$.

As aforementioned, in Cases 3 and 4, the cylinders vibrate in vertical and horizontal directions, respectively. To get a sense of the influence of the vibration amplitude of the cylinders on the average Nusselt number, Figure 17 is presented for four vibrating amplitudes, $L = 0.025$, 0.05, 0.075, and 0.1. Among these amplitudes, $L = 0.05$ provides the highest average Nusselt number for Case 4 while the maximum heat transfer by convection is achieved with $L = 0.075$ in Case 3.

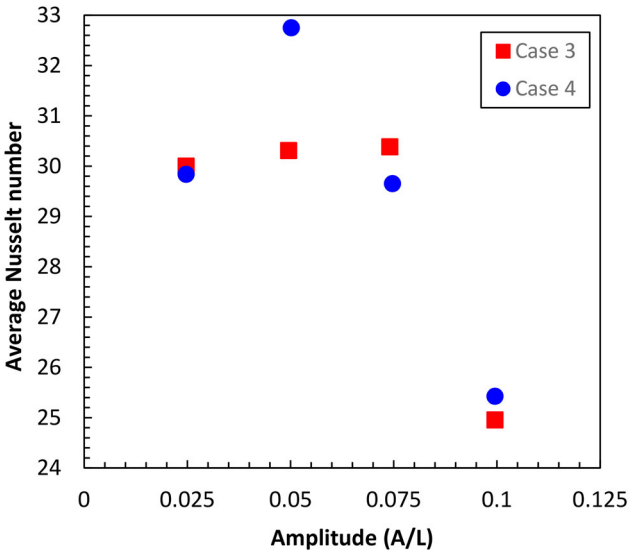

Figure 17. Comparison of average Nusselt number between Cases 3 and 4 with different amplitude at $Re = 150$, $Ri = 100$, $fr = 5$.

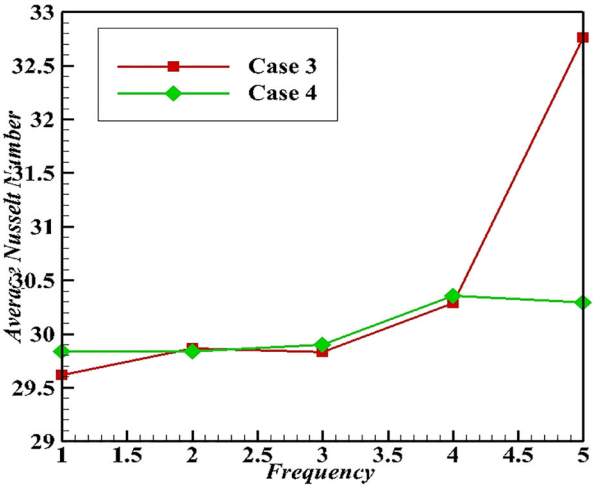

Figure 18. Comparison of average Nusselt number between Cases 3 and 4 with different frequencies at $Re = 150$, $Ri = 100$, $A = 0.05L$.

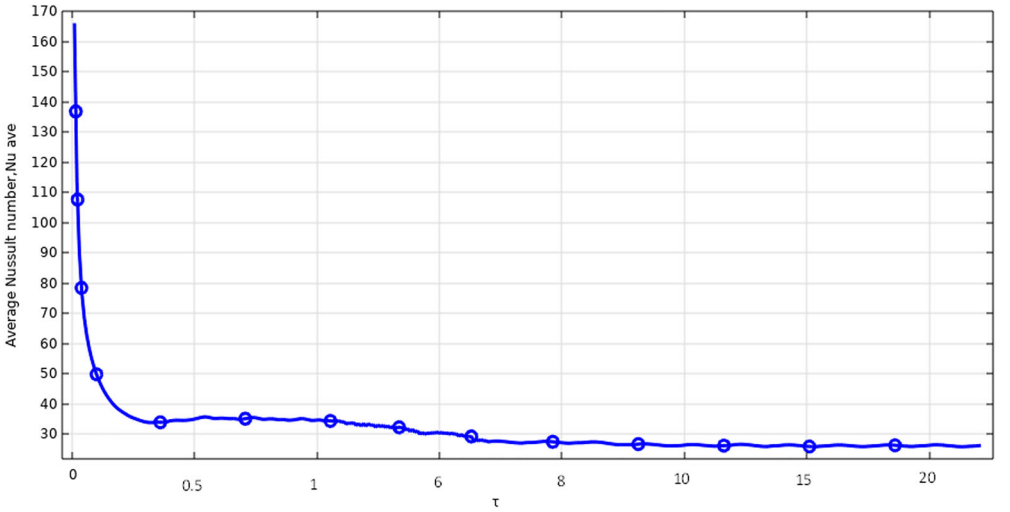

Figure 19. Change in average Nu with time for Case 4, $Re = 150$, $Ri = 100$, $A = 0.05L$, $fr = 5$.

$L = 0.025$ and $L = 0.1$ cause the same heat transfer for Case 3 and 4 while the $L = 0.1$ leads to the minimum regardless of the direction of vibration.

The influence of vibration frequency on heat transfer is shown in Figure 18 by comparing the change in Nusselt number for Case 3 and 4 where all cylinders vibrate with small frequencies in vertical and horizontal directions, respectively. First of all, it can be concluded that any increase in the vibration frequency of the cylinders enhances heat transfer regardless of the direction of the vibrating cylinders in the enclosure. Vibrating the cylinders in vertical and horizontal directions with the frequencies $2 \leq fr \leq 4$ Hz induces almost the same heat transfer. However, when the cylinders vibrate in the vertical direction with $fr > 4$ Hz the Nusselt number increases rapidly which demonstrates the positive influence of the direction and frequency of the vibration on heat transfer by natural convection. The change in Nusselt number with vibration frequency reveals that the $fr = 4$ Hz can be considered as the critical frequency for the problem under consideration because for $fr > 4$ Hz the vibration in the horizontal direction causes a decrease in heat transfer while vibration in the vertical direction increases the Nusselt number when $fr > 4$ Hz.

Heat transfer with mixed convection over time is plotted for Case 4 in Figure 19. It is seen that heat transfer takes place in advance due to the high temperature difference in the flow field. Most of the heat is transferred and the Nusselt number decreases dramatically in the first nondimensional time, $\tau = 0.1$, and then, heat transfer slows down since the Nusselt number decreases very slowly but steadily until $\tau = 7$, and then, it becomes almost constant and does not change with time anymore.

4. Conclusion

In this study, the entropy generation and mixed convection of water flow through a vented enclosure including four cylinders vibrating in the vertical and horizontal directions are considered. The investigations are made for various parameters such as Reynolds and Richardson numbers, the direction of vibration along with the vibration frequency and amplitude and flow time. Upon performing a mesh independence a series of validation studies are successfully performed with two different cases found in the open literature. A linear regression analysis was also applied to reveal the rate at which the average Nusselt number increases with the Reynolds numbers for each case and the Richardson number. The influences of the aforementioned parameters on entropy generation and heat transfer are discussed, and major outcomes are listed below:

- The direction of the vibration of the cylinders influences the flow and temperature fields. Vibration in the vertical direction divides the flowfield into mainly two regions that rotate about the vertical plane while the cylinders vibrate in the horizontal direction such two regions rotate about the horizontal plane.
- The average Nusselt number increases from the Case 1, the enclosure without cylinders to Case 4 in which the cylinders vibrate in the horizontal direction at both Richardson numbers ($Ri = 5$ and 10). It reveals that the existence of the cylinders increases the heat transfer even if the cylinders do not vibrate. The vibration causes higher heat transfer rate as expected while the vibration in the horizontal direction enhances heat transfer rate than the vibration in vertical direction since both the top and bottom walls are adiabatic.
- Entropy generation due to heat transfer can be disregarded at the center of the enclosure. Furthermore, the adiabatic walls do not contribute to entropy generation.
- In the enclosure, without cylinders, the Bejan number does not change considerably with the Reynolds number, however, it is affected by the vibration of cylinders since the irreversibility due to heat transfer occurs.
- The convection heat transfer increases with both Reynolds and Richardson numbers. Linear regression analysis reveals that the average Nusselt number increases at the rate of 0.064285, 0.066761, 0.062482, and 0.064331 for the cases from Case 1 to 4, respectively, due to higher Reynolds number when Richardson number is $Ri = 5$. The average Nusselt number increases at the higher rates when the Reynolds number increases for each case at $Ri = 10$.
- The frequency amplitude of the vibrating cylinders affects the heat transfer phenomenon. The highest Nu is attained for $A = 0.05$L when the cylinders vibrate in the horizontal direction. However, the optimum amplitude is found as $L = 0.075$L when cylinders vibrate in the vertical direction. $A = 0.1$L seems the most unsuitable amplitude, no matter the direction of the cylinders.
- In general, increasing vibration frequency enhances heat transfer regardless of the direction of the vibration of the cylinders. The vibration frequency $fr = 4$ Hz can be considered critical because at $fr > 4$ Hz the magnitude of the average Nu changes with increasing frequency. The Nusselt number increases rapidly with increasing the frequency when they vibrate in the

vertical direction while the Nusselt number changes inversely with increasing the vibration frequency when they vibrate in the horizontal direction.

- Due to the large temperature gradient natural heat transfer occurs in the first nondimensional time $t = 0.1$, and then, it continues as state steady.

Competing interest

We confirm that there are no relevant financial competing interests to report.

ORCID

Mushtaq F. Almensoury http://orcid.org/0000-0002-6782-6662
Seyfettin Bayraktar http://orcid.org/0000-0002-1554-353X
Müslüm Arıcı http://orcid.org/0000-0002-3397-2215

References

[1] M. H. Park and J. H. Lee, "Turbulent natural convection flow and heat transfer in an inclined square enclosure," *KSME J.*, vol. 6, no. 1, pp. 16–23, 1992. DOI: 10.1007/BF02954459.

[2] A. H. Mahmoudi, M. Shahi and F. Talebi, "Entropy generation due to natural convection in a partially open cavity with a thin heat source subjected to a nanofluid," *Numer. Heat Transf. A*, vol. 61, no. 4, pp. 283–305, 2012. DOI: 10.1080/10407782.2012.647990.

[3] P. Moodley, "1 - Sustainable biofuels: Opportunities and challenges," in *Applied Biotechnology Reviews, Sustainable Biofuels*, R. C. Ray, Ed. Academic Press, 2021, pp. 1–20. DOI: 10.1016/B978-0-12-820297-5.00003-7.

[4] P. Moodley and C. Trois, "2 - Lignocellulosic biorefineries: The path forward," in *Applied Biotechnology Reviews, Sustainable Biofuels*, R. C. Ray, Ed. Academic Press, 2021, pp. 21–42. DOI: 10.1016/B978-0-12-820297-5.00010-4.

[5] T. N. Abdelhameed, "Entropy generation analysis for MHD flow of water past an accelerated plate," *Sci. Rep.*, vol. 11, no. 1, pp. 11964, 2021. DOI: 10.1038/s41598-021-89744-w.

[6] Z. M. Mburu, S. Mondal, P. Sibanda, and R. A. Sharma, "A numerical study of entropy generation on oldroyd-B nanofluid flow past a riga plate," *J. Therm. Eng.*, vol. 7, no. 4, pp. 845–866, 2021. DOI: 10.18186/thermal.930653.

[7] W. S. Fu, C. S. Cheng, and W. J. Shieh, "Enhancement of natural convection heat transfer of an enclosure by a rotating circular cylinder," *Int. J. Heat Mass Transf.*, vol. 37, no. 13, pp. 1885–1897, 1994. DOI: 10.1016/0017-9310(94)90329-8.

[8] L. B. Erbay, Z. Altac, and B. Sulus, "Entropy generation in a square enclosure with partial heating from a vertical lateral wall," *Heat Mass Transf.*, vol. 40, no. 12, pp. 909–918, 2004. DOI: 10.1007/s00231-003-0497-x.

[9] M. Sheikholeslami, R. Ellahi, M. Hassan, and S. Soleimani, "A study of natural convection heat transfer in a nanofluid filled enclosure with elliptic inner cylinder," *Int. J. Numer. Methods Heat Fluid Flow*, vol. 24, no. 8, pp. 1906–1927, 2014. DOI: 10.1108/HFF-07-2013-0225.

[10] Y. F. Wang *et al.*, "Laminar mixed convection heat transfer of SiC-EG nanofluids in a triangular enclosure with a rotating inner cylinder: Simulations based on the measured thermal conductivity and viscosity," *J. Zhejiang Univ. Sci. A*, vol. 16, no. 6, pp. 478–490, 2015. DOI: 10.1631/jzus.A1400120.

[11] A. I. Alsabery, T. Tayebi, R. Roslan, A. J. Chamkha, and I. Hashim, "Entropy generation and mixed convection flow inside a wavy-walled enclosure containing a rotating solid cylinder and a heat source," *Entropy*, vol. 22, no. 6, pp. 606, 2020. DOI: 10.3390/e22060606.

[12] K. Yazdani, M. Sahebjamei, and A. Ahmadpour, "Natural convection heat transfer and entropy generation in a porous trapezoidal enclosure saturated with power-law non-Newtonian fluids," *Heat Transf. Eng.*, vol. 41, no. 11, pp. 982–1001, 2020. DOI: 10.1080/01457632.2019.1589993.

[13] S. Dutta, N. Goswami, S. Pati, and A. K. Biswas, "Natural convection heat transfer and entropy generation in a porous rhombic enclosure: Influence of non-uniform heating," *J. Therm. Anal. Calorim.*, vol. 144, no. 4, pp. 1493–1515, 2021. DOI: 10.1007/s10973-020-09634-7.

[14] R. Lemlich, "Effect of vibration on natural convective heat transfer," *Ind. Eng. Chem.*, vol. 47, no. 6, pp. 1175–1180, 1955. DOI: 10.1021/ie50546a024.

[15] R. M. Russ, "Effect of vibration on heat transfer from cylinders in free convection," M.Sc. thesis, Faculty of the School of Engineering of the Air Force Institute of Technology, Air University, 1962.

[16] J. M. Faircloth and W. J. Schaetzle, "Effect of vibration on heat transfer for flow normal to a cylinder," *J. Heat Transf.*, vol. 91, no. 1, pp. 140–144, 1969. DOI: 10.1115/1.3580070.
[17] K. K. Prasad and V. Ramanathan, "Heat transfer by free convection from a longitudinally vibrating vertical plate," *Int. J. Heat Mass Transf.*, vol. 15, no. 6, pp. 1213–1223, 1972. DOI: 10.1016/0017-9310(72)90186-X.
[18] H. Kimoto, A. Kadotsuji, and T. Hirose, "Effect of vibration on the natural convection heat transfer of a horizontal cylinder," *Bull. JSME*, vol. 26, no. 217, pp. 1154–1161, 1983. DOI: 10.1299/jsme1958.26.1154.
[19] M. A. Shalaby, E. A. Elnegiry, and H. R. El-Tahan, "Forced convection heat transfer from oscilating horizontal cylinder," *Mansoura Eng. J.*, vol. 28, no. 4, pp. 1–14, 2021. DOI: 10.21608/bfemu.2021.142396.
[20] W. S. Fu and W. J. Shieh, "A study of thermal convection in an enclosure induced simultaneously by gravity and vibration," *Int. J. Heat Mass Transf.*, vol. 35, no. 7, pp. 1695–1710, 1992. DOI: 10.1016/0017-9310(92)90140-N.
[21] W. S. Fu and W. J. Shieh, "Transient thermal convection in an enclosure induced simultaneously by gravity and vibration," *Int. J. Heat Mass Transf.*, vol. 36, no. 2, pp. 437–452, 1993. DOI: 10.1016/0017-9310(93)80019-Q.
[22] W. S. Fu and C. P. Huang, "Effects of a vibrational heat surface on natural convection in a vertical channel flow," *Int. J. Heat Mass Transf.*, vol. 49, no. 7–8, pp. 1340–1349, 2006. DOI: 10.1016/j.ijheatmasstransfer.2005.10.028.
[23] P. Xie and X. Zhang, "Study of laminar convection heat transfer in single-side-heating small-scale cooling channel with vibrating cylinder," *Int. Commun. Heat Mass Transf.*, vol. 120, pp. 105030, 2021. DOI: 10.1016/j.icheatmasstransfer.2020.105030.
[24] M. M. Al-Azzawi, A. R. Abdullah, B. M. Majel, and L. J. Habeeb, "Experimental investigation of the effect of forced vibration on natural heat transfer in a concentric vertical cylinder," *J. Mech. Eng. Res. Dev.*, vol. 44, no. 3, pp. 56–65, 2021.
[25] V. Kozlov, K. Rysin, and A. Vjatkin, "Vibroconvective patterns in a layer under translational vibrations of circular polarization," *Fluids*, vol. 6, no. 3, pp. 108, 2021. DOI: 10.3390/fluids6030108.
[26] S. Sivasankaran, V. Sivakumar, and A. K. Hussein, "Numerical study on mixed convection in an inclined lid-driven cavity with discrete heating," *Int. Commun. Heat Mass Transf.*, vol. 46, pp. 112–125, 2013. DOI: 10.1016/j.icheatmasstransfer.2013.05.022.
[27] I. I. Nosonov and M. A. Sheremet, "Conjugate mixed convection in a rectangular cavity with a local heater," *Int. J. Mech. Sci.*, vol. 136, pp. 243–251, 2018. DOI: 10.1016/j.ijmecsci.2017.12.049.
[28] W. Cao, I. L. Animasaun, S. J. Yook, V. A. Oladipupo, and X. Ji, "Simulation of the dynamics of colloidal mixture of water with various nanoparticles at different levels of partial slip: Ternary-hybrid nanofluid," *Int. Commun. Heat Mass Transf.*, vol. 135, pp. 106069, 2022. DOI: 10.1016/j.icheatmasstransfer.2022.106069.
[29] H. M. Blackburn and R. D. Henderson, "A study of two-dimensional flow past an oscillating cylinder," *J. Fluid Mech.*, vol. 385, pp. 255–286, 1999. DOI: 10.1017/S0022112099004309.
[30] A. Islam, M. D. Rony, M. Islam, E. H. Chowdhury, and M. N. Hasan, "Mixed convective heat transfer enhancement in a ventilated cavity by flow modulation via rotating plate," *Heat Transf.*, vol. 50, no. 3, pp. 2339–2361, 2021. DOI: 10.1002/htj.21981.
[31] A. Roshko, "Experiments on the flow past a circular cylinder at very high Reynolds number," *J. Fluid Mech.*, vol. 10, no. 3, pp. 345–356, 1961. DOI: 10.1017/S0022112061000950.
[32] O. Lehmkuhl, L. Rodríguez, R. Borrell, J. Chiva, and A. Oliva, "Unsteady forces on a circular cylinder at critical Reynolds numbers," *Phys. Fluids*, vol. 26, no. 12, pp. 125110, 2014. DOI: 10.1063/1.4904415.
[33] A. Bejan, *Entropy Generation Minimization*. USA: CRC Press, 1966.
[34] S. V. Patankar, *Numerical Heat Transfer and Fluid Flow*. New York: McGraw-Hill, 1980.
[35] A. Maougal and R. Bessaih, "Heat transfer an entropy analysis for mixed convection in a discretely heated porous square cavity," *Fluid Dyn. Mater. Process.*, vol. 9, no. 1, pp. 35–59, 2013. DOI: 10.3970/fdmp.2013.009.035.
[36] A. J. Chamkha, S. H. Hussain, and Q. R. Abd-Amer, "Mixed convection heat transfer of air inside a square vented cavity with a heated horizontal square cylinder," *Numer. Heat Transf. A*, vol. 59, no. 1, pp. 58–79, 2011. DOI: 10.1080/10407782.2011.541216.
[37] M. Nallasamy and K. K. Prassad, "On the cavity flow at high Reynolds numbers," *J. Fluid Mech.*, vol. 79, no. 2, pp. 391–414, 1977. DOI: 10.1017/S0022112077000214.
[38] J. Zhang, B. Xiao, and W. Yang, "Numerical study of lid-driven square cavity flow with embedded circular obstacles using spectral/hp element methods," *Appl. Sci.*, vol. 12, no. 22, pp. 11711, 2022. DOI: 10.3390/app122211711.
[39] M. M. Rahman *et al.*, "Effects of Reynolds and Prandtl number on mixed convection in a ventilated cavity with a heat-generating solid circular block," *Appl. Math. Model.*, vol. 36, no. 5, pp. 2056–2066, 2012. DOI: 10.1016/j.apm.2011.08.014.

[40] A. Yasin, N. Ullah, S. Nadeem, and H. A. Ghazwani, "Numerical simulation for mixed convection in a parallelogram enclosure: Magnetohydrodynamic (MHD) and moving wall-undulation effects," *Int. Commun. Heat Mass Transf.*, vol. 135, pp. 106066, 2022. DOI: 10.1016/j.icheatmasstransfer.2022.106066.

[41] N. Shirani and D. Toghraie, "Numerical investigation of transient mixed convection of nanofluid in a cavity with non-Darcy porous inner block and rotating cylinders with harmonic motion," *Sci. Rep.*, vol. 11, no. 1, pp. 17281, 2021. DOI: 10.1038/s41598-021-96733-6.

[42] S. S. Arasavelli, R. Konijeti, and G. R. Budda, "Positive impact of vibration on heat transfer in twisted tape inserted heat exchanger," *J. Therm. Eng.*, vol. 7, no. 7, pp. 1731–1742, 2021. DOI: 10.18186/thermal.1025962.

[43] M. Ghalambaz, E. Jamesahar, M. A. Ismael, and A. J. Chamkha, "Fluid-structure interaction study of natural convection heat transfer over a flexible oscillating fin in a square cavity," *Int. J. Therm. Sci.*, vol. 111, pp. 256–273, 2017. DOI: 10.1016/j.ijthermalsci.2016.09.001.

[44] M. Roy, T. Basak, S. Roy, and I. Pop, "Analysis of entropy generation for mixed convection in a square cavity for various thermal boundary conditions," *Numer. Heat Transf. A*, vol. 68, no. 1, pp. 44–74, 2015. DOI: 10.1080/10407782.2014.955352.

[45] S. Soleimani, A. Qajarjazi, H. Barari, A. Barari, and G. Domairry, "Entropy generation due to natural convection in a partially heated cavity by local RBF-DQ method," *Meccanica*, vol. 46, no. 5, pp. 1023–1033, 2011. DOI: 10.1007/s11012-010-9358-0.

[46] S. M. H. Zadeh, S. A. M. Mehryan, M. S. Islam, and M. Ghalambaz, "Irreversibility analysis of a thermally driven flow of a water-based suspension with dispersed nano-sized capsules of phase change material," *Int. J. Heat Mass Transf.*, vol. 155, pp. 119796, 2020. DOI: 10.1016/j.ijheatmasstransfer.2020.119796.

[47] I. L. Animasaun *et al.*, *Ratio of Momentum Diffusivity to Thermal Diffusivity: Introduction, Meta-Analysis, and Scrutinization*. New York: Chapman and Hall/CRC, 2022.

[48] S. Saleem *et al.*, "Insight into the motion of water conveying three kinds of nanoparticles shapes on a horizontal surface: Significance of thermo-migration and Brownian motion," *Surf. Interfaces*, vol. 30, pp. 101854, 2022. DOI: 10.1016/j.surfin.2022.101854.

[49] I. L. Animasaun, R. O. Ibraheem, B. Mahanthesh, and H. A. Babatunde, "A meta-analysis on the effects of haphazard motion of tiny/nano-sized particles on the dynamics and other physical properties of some fluids," *Chin. J. Phys.*, vol. 60, pp. 676–687, 2019. DOI: 10.1016/j.cjph.2019.06.007.